This is a non-peer-reviewed preprint submitted to EarthArXiv and currently under review in Frontiers in Environmental Science - Biogeochemical Dynamics.

Reframing natural organic matter research through compositional data analysis

Morimaru Kida[1,*], Julian Merder[2,a], Thorsten Dittmar[3,4], Vera Pawlowsky-Glahn[5], and Juan José Egozcue[6]

[1]Soil Science Laboratory, Graduate School of Agricultural Science, Kobe University, 1-1 Rokkodai, Nada, Kobe, Hyogo 657-8501, Japan,
[2]Department of Global Ecology, Carnegie Institution for Science, 260 Panama Street, Stanford, CA 94305, USA
[3]Institute for Chemistry and Biology of the Marine Environment (ICBM), School of Mathematics and Science, University of Oldenburg, Oldenburg, Germany
[4]Helmholtz Institute for Functional Marine Biodiversity at the University of Oldenburg (HIFMB), Oldenburg, Germany
[5]Department of Computer Sciences, Applied Mathematics, and Statistics, Universitat de Girona, Campus Montilivi, P4, 17003 Girona, Spain
[6]Department of Civil and Environmental Engineering, Universitat Politécnica de Catalunya, Jordi Girona 1-3, Mod. C2, 08034 Barcelona, Spain
[a]Present address: School of Biological Sciences, University of Canterbury, Private Bag 4800, Christchurch 8140, New Zealand

October 13, 2025

*Corresponding Author: **Morimaru Kida**, Soil Science Laboratory, Graduate School of Agricultural Science, Kobe University, 1-1 Rokkodai, Nada, Kobe, Hyogo 657-8501, Japan. morimaru.kida@people.kobe-u.ac.jp

Abstract

Compositional data (CoDa) are prevalent in environmental research. They represent parts of a whole, such as percentages, proportions, and relative or absolute abundance. They are arrays of positive data that convey relevant information in the ratios between their components. Standard statistical techniques developed for real random observations often yield spurious results and are therefore unsuitable for CoDa, which has unique geometric properties. CoDa analysis is now widely acknowledged across various research fields, ranging from geoscience to social science, with a recent surge in popularity in microbial genomics. However, its adoption remains limited in natural organic matter (NOM) research, despite NOM data from key analytical tools such as mass spectrometry, fluorescence spectroscopy, and nuclear magnetic resonance spectroscopy all being compositional. Given the structural similarity between NOM and high-throughput sequencing data, for which CoDa analysis has been successfully adopted, we argue that CoDa analysis should also be consistently integrated into NOM research to prevent analytical pitfalls and misleading inferences. A few pioneering studies have applied CoDa analysis to NOM data, and a wide array of useful open-source tools are already available. This paper discusses step-by-step the application of CoDa analysis to NOM research, using ultrahigh-resolution mass spectrometry data as an illustrative example. The goal of the study is to provide the community with an overview of CoDa analysis and guide them on how to use it in practice.

Keywords: CoDa, FT-ICR MS, NMR, Orbitrap mass spectrometry, EEM, PARAFAC, sum constraint.

1 Introduction

Natural organic matter (NOM) exists ubiquitously in soil and water and comprises a diverse mixture of organic molecules. Because of its diverse composition featuring reactive functional groups, NOM serves multiple roles in the environment, including rock weathering (Chadwick and Chorover, 2001), photochemistry (Arts et al., 2000), metal speciation or toxicity (Muller and Cuscov, 2017; Taylor et al., 2016), microbial metabolism (Tranvik, 1992), and carbon storage (Hedges et al., 1997). Molecular characterisation of NOM has been conducted to mechanistically understand the link between these roles and their molecular composition. Techniques proven particularly successful include excitation-emission matrix spectroscopy combined with parallel factor analysis (EEM-PARAFAC) (Stedmon et al., 2003), high-field nuclear magnetic resonance spectroscopy (NMR)

(Baldock et al., 1997; Mao et al., 2017; Hertkorn et al., 2013), and ultra high-resolution mass spectrometry, such as Fourier-transform ion cyclotron resonance mass spectrometry (FT-ICR MS) (Koch et al., 2005; Kujawinski et al., 2002). These techniques are frequently employed to understand the dynamics of specific organic compounds or compound groups (hereafter referred to as "compounds" for simplicity) and their role in ecological functions.

Two major challenges exist in analysing and interpreting the data sets generated by these molecular techniques. First, each technique exhibits specificity toward or against certain compounds, and the data obtained reflect the integral consequence of sample treatment (e.g., solid-phase extraction) and analysis (e.g., ionisation efficiency), alongside true variation in the ecosystem. These analytical aspects are well-acknowledged, and sufficient knowledge and careful data evaluation can mitigate biased interpretations (Konermann et al., 2013; Mao et al., 2017; Murphy et al., 2010; Perminova et al., 2014). Second, there is a constraint on the data structure imposed either by the sample size, instrumental capacity, or mathematically, representing a significant, yet often unrecognised, mathematical challenge in NOM research. Absolute abundance of analytes always has an upper limit constrained by the sample size or sampling design because it is never possible to measure an infinitely large sample (Gloor et al., 2017). In addition, a fixed upper bound on the total instrumental signal also imposes a constraint. For instance, the ion trap of FT-ICR MS can store a fixed amount of ions at a given time; thus, increases in given ions will decrease other ions when the trap is filled to near limit, albeit not very strictly or predictably compared to the "library size" of sequencing data. This constraint on the data structure by instrumental capacity has also been illustrated in high-throughput sequencing (Gloor and Reid, 2016). Although this effect may be avoided by limiting the sample loading or adjusting the ion accumulation time per sample, controlling for it is not always possible or practical. We will explain in Section 2 how this constraint can be alleviated using ratios between data components. Contrarily, relative abundance, normalised by the total signal intensity of the sample, sums up to a constant (e.g., 1 or 100) and has an obvious mathematical constraint. Thus, these data are always compositional data (CoDa).

Compositional data are characterised as arrays of positive data conveying relevant information in the ratios between their components (Aitchison, 1982; Pawlowsky-Glahn et al., 2015; Greenacre, 2021). This fact suggests considering them as *equivalence classes* that can be represented in different ways (Aitchison, 1992; Barceló-Vidal and Martín-Fernández, 2016). In other words, the key idea underlying CoDa analysis is that the compositional information conveyed by CoDa does not change when it is multiplied by a positive constant (*the principle of scale invariance*) (Aitchison, 1982). This implies that absolute and the corresponding relative abundances carry the same compositional information. Examples of rep-

resentations of CoDa in environmental science include measurements of the absolute or relative abundances, proportions, or percentages of components in a single sample. Geometrically, CoDa can be represented as confined to the *simplex* and are not freely distributed in the *real Euclidean space* (Egozcue and Pawlowsky-Glahn, 2018). For instance, CoDa with three parts can be represented inside a triangle, while those with four parts within a tetrahedron, and so forth. Importantly, the simplex contains one less dimension than the number of components. Furthermore, the ordinary sum and difference of CoDa lose their roles in the simplex because the results can no longer be compositions in the simplex. These geometric properties of CoDa mean that standard statistical techniques developed for *real random data* (that is, data possibly distributed from negative to positive infinity on an absolute scale) are inherently inapplicable to CoDa.

Relative data are often reported in NOM research due to analytical limitations. For instance, in FT-ICR MS analysis, obtaining the same overall measured mass signal across a dataset is virtually impossible, even when using the identical mass spectrometer under the same instrumental settings. This variability may stem from technical difficulties in precisely preparing sample concentrations and injecting the same volume, variations in ionisation efficiency among samples, or both. To account for possible differences in the overall intensities, mass spectra intensities are usually normalised (called *closed* in CoDa analysis) or reported as relative intensities. The relative intensities of mass spectra within a sample must sum to a constant value, meaning that changes in one peak's intensity will reciprocally affect others. This is referred to as *constant-sum constraint*, which can lead to *negative correlation bias* and violates the assumption of variable independence in many statistical analyses (Chayes, 1960; Aitchison, 1986). In other words, relative intensities of a mass spectrum are mutually dependent features that cannot be understood in isolation. Consequently, basic statistical measures like mean and variance are inadequate under this constraint (Filzmoser et al., 2009), and correlations between data components can change depending on which components of the whole are considered in the analysis (Lovell et al., 2015). This phenomenon, termed *subcompositional incoherence* (see Section 3.2) (Aitchison and Egozcue, 2005; Egozcue and Pawlowsky-Glahn, 2023), highlights that correlations between peak pairs can shift based on the subset of mass peaks considered. In CoDa analysis, the whole data is termed *composition* (not to be confused with the term molecular composition), and its components are called *parts*. This term was introduced by the founder of CoDa analysis, John Aitchison, to avoid confusion with random variables, which are considered to be, by definition, *real*, implying that their sample space is the whole real line, from $-\infty$ to $+\infty$, endowed with the usual Euclidean geometry on an absolute scale. This assumption does not hold for CoDa and is the underlying reason for spurious correlation, negative bias, and subcompositional incoherence.

Fortunately, specific methods for addressing compositional challenges have already been developed within CoDa analysis and have demonstrated utility across various disciplines, including geosciences (Egozcue et al., 2024), sedimentology (Tolosana-Delgado, 2012), genomics (Gloor et al., 2017), proteomics (O'Brien et al., 2018), epidemiology (Dumuid et al., 2020), and social science (Gupta et al., 2018), to name but a few. A compositional approach has also been applied to specific molecular characterisation techniques such as NMR (Abdi et al., 2015) and mass spectrometry (Graeve and Greenacre, 2020). Several software packages for *R* (`https://www.r-project.org/`) are also available (Boogaart and Tolosana-Delgado, 2013; Boogaart and Tolosana-Delgado, 2008; Gloor, 2023; Palarea-Albaladejo and Martín-Fernández, 2015; Quinn et al., 2017; Frerebeau and Philippe, 2025), easing the learning curve for novices. Given the transformative impact of a single tutorial/perspective paper on the analysis of high-throughput sequencing data using compositional methods (Gloor et al., 2017), we anticipate that CoDa analysis will inevitably be incorporated into NOM research, considering the similarity of data structures discussed later. Already, a few pioneering studies have applied CoDa analysis to NOM data (Fonvielle et al., 2021; Kida et al., 021a,b, 2025; Osterholz et al., 2022; Hu et al., 2022).

In Section 2, we will briefly explain how the distance between CoDa should be measured because it is different from Euclidean distance, and distance measures are fundamental to any statistics. In Section 3, we will discuss the application of CoDa analysis in NOM research, using FT-ICR MS data as an illustrative example. This discussion can be extended to virtually all analytical instruments that generate signal or peak intensities analysed or reported on a relative scale. The challenges encountered when CoDa is analysed using non-compositional methods have been extensively reviewed across diverse scientific disciplines (Aitchison and Egozcue, 2005; Egozcue et al., 2024; Filzmoser et al., 2009; Gloor et al., 2017; Kida et al., 021b; Reimann et al., 2012; Templ and Templ, 2020). The theoretical and mathematical foundations are covered in several books (see, e.g., Pawlowsky-Glahn et al., 2015; Filzmoser et al., 2018) building on a pioneering work by Aitchison (1986). Therefore, we will focus on the practical aspects of working with FT-ICR MS data, as CoDa, and provide effective approaches to guide the reader. We will limit our discussion to data analysis; the theoretical factors that influence the response and identification of compounds in FT-ICR MS analysis are well understood (Qi et al., 2022; Bahureksa et al., 2021; Hawkes et al., 2020) and are outside the scope of this paper.

2 Distances between compositional data and advantages of taking ratios

The starting point for any compositional analysis is a ratio transformation of the data, as illustrated in the analysis of sequencing data (Gloor et al., 2017) (Fig. 1) (see Supplementary Introduction for mathematical background). Ratios remain constant regardless of data normalisation or subsetting, making them a natural solution for handling CoDa (see Section 3.2 Correlation by peak intensities). Ratios are generally compared multiplicatively (Isles, 2020), so the logarithmic transformation converts the ratios from a multiplicative scale to an additive scale (i.e., from a ratio scale to an interval scale) (Greenacre, 2021). Frequently, the logarithm of ratios (*logratios*) is taken to make the data look symmetric, but in the present context, it is taken to move them from a representation in the simplex into a representation in the *real space* (Aitchison et al., 2000; Pawlowsky-Glahn and Egozcue, 2001). Logratios comply with standard statistical methods developed for real random variables, albeit with special interpretability issues in analytical outcomes (Aitchison et al., 2000; Greenacre, 2021) (see Supplementary Discussion 2.2 for the result of the principal component analysis).

Several methods exist for computing ratios between compositional variables, including additive logratio (alr) (Aitchison, 1982), centred logratio (clr) (Aitchison, 1986), and isometric or orthonormal logratio (ilr or olr) (Egozcue et al., 2003; Egozcue and Pawlowsky-Glahn, 2005; Martín-Fernández, 2019). Also, principal components for CoDa produce ilr/olr logratio coordinates. (Fig. 1, Table 1).

The alr transformation is the logarithm of the ratio of each part over a common part in the composition, as the denominator; thus, analysis of elemental ratios, such as H/C and O/C, can be reframed in a unified context of CoDa analysis. However, as the alr transformation is not an isometric transformation from the simplex, endowed with the Aitchison geometry (Pawlowsky-Glahn and Egozcue, 2001), onto the real space with the ordinary Euclidean metric, the Euclidean distance between alr-transformed data loses meaning. In other words, the alr-transformed data can only be analysed by classical multivariate analysis tools not relying on a distance. However, with a careful selection of the reference denominator, it is possible to make it close to being isometric in some particular cases (Greenacre et al., 2021). We provide this possibility in Supplementary Discussion 2.3.

The clr transformation is the most widely used and most convenient for computational purposes because clr transformation is isometric and provides a one-to-one transformation. The clr-transformed data can readily be used for standard statistical methods (Greenacre, 2021) when not relying on a full rank of the covariance (not based on covariance or correlation matrices), as clr-transformed data sum up to zero. A clr is the logratio between a part and the geometric mean of

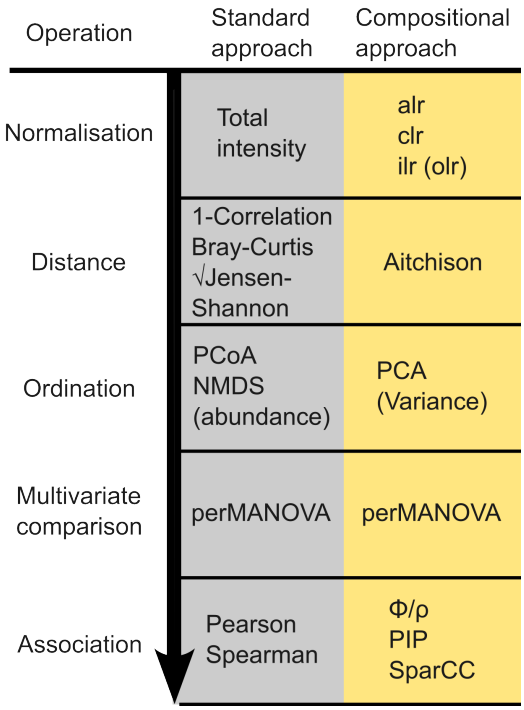

Figure 1: **The standard analysis tool kit for natural organic matter research and the compositional replacements.** The initial normalisation steps are not formally equivalent since compositional data are inherently "normalised", and total signal normalisation is unnecessary. The other steps are functionally related and substitute a compositionally appropriate approach for one that is not. Notation: alr, clr, ilr or olr = additive, centred, isometric or orthonormal log ratio. PIP = proportionality index of parts. Figure and caption modified from Gloor et al. (2017) under the terms of the CC BY.

all D parts in the composition (Aitchison, 1986). Thus, the original data in a D-dimensional constrained space is clr-transformed by:

$$\mathrm{clr}(\mathbf{x}) = \left(\ln \frac{x_1}{\mathrm{g_m}(\mathbf{x})}, \ln \frac{x_2}{\mathrm{g_m}(\mathbf{x})}, \ldots \ln \frac{x_D}{\mathrm{g_m}(\mathbf{x})} \right), \qquad \mathrm{g_m}(\mathbf{x}) = \prod_{i=1}^{D} x_i^{1/D} \quad . \tag{1}$$

A clr-component thus represents the logarithm of a part which is centred with respect to the mean of the logarithms of all parts in the sample. In other words, a clr should not be interpreted independently but always relative to all other features of the data set. One of the most common mistakes is to compute the correlation between two clr components and to interpret it as if it were the correlation between the two parts in the numerator *per se*. See Egozcue and Pawlowsky-Glahn (2023) for details on related problems. The distance between compositional variables in the simplex is measured by the *Aitchison distance* (Aitchison, 1986) (Fig. 1). Conveniently, the Aitchison distance is simply the Euclidean distance between the

Table 1: Summary of common data transformations in compositional data analysis.

Transformation / coordinates	Merit / Pros	Demerit / Cons
alr, direct computation Aitchison (1982)	Simple; sometimes aligns with traditional indices (e.g., H/C, O/C); subcompositionally coherent.	Not isometric; the interpretation of the transformed data is not intuitive; requires a reference part.
clr, direct computation Aitchison (1983)	Isometric; one-to-one transformation; choice for almost all classical multivariate analyses; efficiently used in many computations.	Transformed variables sum up to zero; in each component, all parts are involved; resulting covariance matrix is always singular; subcompositionally incoherent; correlation is spurious.
ilr(olr), sequential binary partition Egozcue and Pawlowsky-Glahn (2005)	Allows user-defined partition which can align with traditional indices (e.g., H/C, O/C); coordinates are balances; choice for all classical multivariate analysis; provides orthogonal Cartesian coordinates.	Interpretation based on geometric means of groups of parts; manually building partitions for high-dimensional data is tedious.
ilr(olr), CoDa Principal Components Aitchison (1984)	Data-driven selection of basis; coordinates ordered by variance; choice for all classical multivariate analyses; appropriate for biplots; provides orthogonal Cartesian coordinates.	Principal coordinates are general log-contrasts involving all parts; difficulties for simplification.
ilr(olr), CoDa Principal Balances Martín-Fernández et al. (2018)	Data-driven selection of basis. Coordinates are balances; coordinates ordered by variance; choice for all classical multivariate analyses; appropriate for biplots; provides orthogonal Cartesian coordinates.	Interpretation of geometric means of groups of parts.

clr-transformed data, which is why clr-transformed data are useful in the computation of statistical methods. The Aitchison distance is superior to the commonly used Bray-Curtis dissimilarity due to its greater robustness against data subsetting and aggregation (Bian et al., 2017; Wong et al., 2016), representing a true linear distance for CoDa (Aitchison et al., 2002; Gloor et al., 2017).

The *isometric log-ratio transformations* ilr (Egozcue et al., 2003), also known as orthogonal log-ratio olr (Martín-Fernández, 2019), provide orthogonal Cartesian coordinates to deal with CoDa in a framework of a *Euclidean Space* (Pawlowsky-Glahn and Egozcue, 2001). The coordinates can be treated as in the elementary geometric way in the real space, and standard statistical procedures can be applied to those ilr coordinates without restriction (Mateu-Figueras et al., 2011). There are several ways to obtain ilr coordinates, the first introduced one being the *CoDa-Principal Components* (Aitchison, 1983), a data-driven procedure. CoDa-Principal Components were defined before the concept of orthogonal coor-

dinates for CoDa. These coordinates are general scale-invariant log-contrasts and therefore they have a hard interpretation unless they are plotted in CoDa-biplots (Aitchison and Greenacre, 2002). A second procedure to get ilr coordinates is based on a sequential binary partition of parts into groups. It can be designed by the analyst to align with some log-ratios of interest. These coordinates are *balances*, normalised log-ratios of geometric means of parts within groups (Egozcue and Pawlowsky-Glahn, 2005) (equation (3) in Supplementary Information). Although some authors considered this fact as an inconvenience for interpretation, understanding the concept of association of parts (Egozcue et al., 2018; Egozcue and Pawlowsky-Glahn, 2023) in the form of balances allows the analyst to make straightforward interpretations. Balances mimic a *dysbiosis*. Dysbiosis is most commonly reported as a condition in the gastrointestinal tract or plant rhizosphere (Wikipedia, consulted on September 23, 2025). If properly selected, they provide hints to the main differences between the two populations. Finally, the sequential binary partition method can be adapted to a data-driven procedure called *principal balances* (Martín-Fernández et al., 2018). Principal balances try to approach CoDa Principal Components by balances, thus facilitating the interpretation of principal components. The exact procedure is computationally time demanding, but approximate procedures are available, like, for instance, the algorithm presented in SELBAL (Rivera-Pinto et al., 2018).

In the context of FT-ICR MS analysis, using ratios of peak intensities has two important advantages: first, since ratios do not require data normalisation, bias introduced by various normalisation approaches into the data, which has been thoroughly discussed in a recent paper (Thompson et al., 2021), will be avoided. As mentioned in their paper, currently, no consensus normalisation approach for FT-ICR MS exists (e.g., normalisation by the sum of only the molecular formula-assigned peaks or by the sum of all the peaks detected; should isotopologues be included in either case?), but when working with ratios, normalisation is not required from the beginning. Second, the constraint on the data structure by sample size or instrumental capacity, as well as negative correlation bias in relative data, can be alleviated by using logratios. As logratio transformations open the data and effectively remove the distortion in the constrained data, examination of the data after these transformations can provide more robust inferences.

One frequently encountered problem with any log-ratio transformation of CoDa is that it cannot be calculated if there are zeros in the data. Because FT-ICR MS data are zero-laden data, this problem arises immediately when analysing relative intensities. Handling zeros remains a major challenge in CoDa analysis, but fortunately, several approaches have been proposed (Lubbe et al., 2021; Martín-Fernández et al., 2003). These are broadly categorised into three approaches: deleting features with zero values, replacing zeros with reasonably small numbers, or combining related variables to avoid zeros. For replacement, there are

several methods from simple replacement by a sensible value (e.g., a value lower than the detection limit) (Martín-Fernández et al., 2003) to Bayesian approaches (Martín-Fernández et al., 2015; Fernandes et al., 2014). One should always check if the removal or modification of zeros does not alter the overall interpretation of the results. We will discuss this topic briefly in Section 3.2. We refer readers to the literature specifically discussing this topic (Hron et al., 2010; Lubbe et al., 2021; Martín-Fernández et al., 2003; Martín-Fernández et al., 2011; Martín-Fernández et al., 2015; Palarea-Albaladejo and Martín-Fernández, 2015)

3 Worked examples with FT-ICR MS data

One of the global goals of FT-ICR MS analysis of NOM is to mechanistically understand the dynamics of organic compounds in natural or anthropogenic environments and to identify the factors influencing these processes. To this end, relationships between samples or variables are analysed. When time is not involved, data analysis is generally defined as Q or R analysis (Legendre and Legendre, 2012a). In Q analysis, the relationships among samples (objects) are analysed (e.g., principal component analysis), while in R analysis, the relationships among variables (descriptors) are analysed using coefficients such as Pearson's *r* correlation coefficient, hence the term R analysis (e.g., correlation or network analysis and regression analysis). The distinction between these modes of analysis is not always immediately clear. Following Legendre and Legendre (2012a), we define analyses that begin with the computation of an association matrix among objects as Q analyses, while those that start with the computation of an association matrix among descriptors are referred to as R analyses. Importantly, these modes of analysis use different measures of association, a distinction that is also critical in CoDa analysis. In the following sections, we present examples of both Q and R analyses.

3.1 General characteristics of data

We will use an openly available dataset from an online data repository (`https://doi.pangaea.de/10.1594/PANGAEA.956291`). This dataset consists of the relative peak intensities of 9910 mass peaks from 48 Antarctic lakes analysed by 15 T FT-ICR MS solariX XR (Bruker Daltonik, Bremen, Germany) (Kida et al., 2023), with each mass peak assigned a molecular formula. Before starting discussions on CoDa analysis, we will explain the general characteristics of the data to help us understand its nature. First, FT-ICR MS data can be described as left-censored, sparse data with the rest of the entries strictly positive. In our example, not all mass peaks were present in all samples, and the number of molec-

ular formulae detected per sample ranged from 2121 to 6338 (Kida et al., 2023). When a molecular formula was not detected in a sample, its relative abundance was recorded as zero, a common way to handle FT-ICR MS data of NOM. Consequently, each sample contained between 3572 and 7789 zeros due to undetected molecular formulae. That a molecular formula was not detected means that the intensity of the mass peak of that molecular formula was not high enough to distinguish it from the noise with a certain level of confidence (Riedel and Dittmar, 2014). In this regard, the zeros of the FT-ICR MS data can be considered as *rounded zeros* that occur when continuous variables fall below the detection limit of the instrument (Martín-Fernández et al., 2003).

Second, the distribution of molecular formulae detected by FT-ICR MS across samples often shows significant unevenness, as evidenced by cumulative counts and rank abundance curves (Fig. 2). Depending on the type of lake, the number of molecular formulae detected differed considerably, with more unique molecular formulae observed as more lakes were analysed (Fig. 2a). The rank abundance curve indicated the presence of ubiquitous molecular formulae with high relative abundance and many others with lower relative abundance (Fig. 2b). Approximately 15% of molecular formulae represented 75% of the relative abundance (Fig. 2c), a typical pattern observed in NOM (Kellerman et al., 2014).

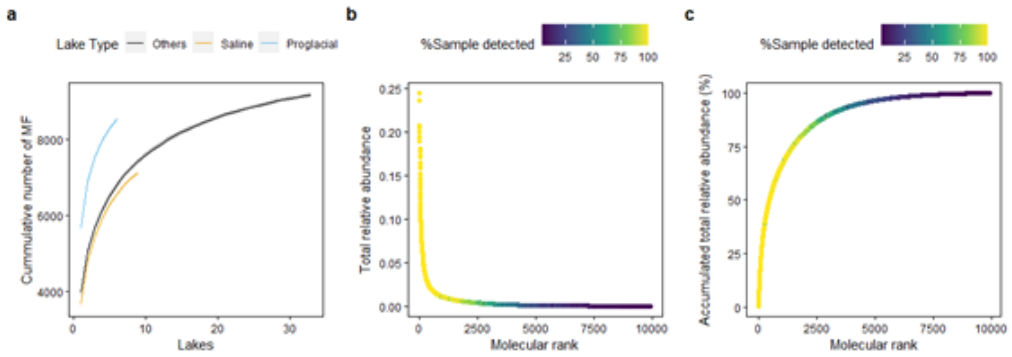

Figure 2: **Distributions of molecular formulae detected by FT-ICR MS in an exemplary dataset from Antarctic lakes** (Kida et al., 2023). (a) Number of unique molecule formulae with each added lake, depending on lake types. Confidence intervals are calculated over 1,000 permutations, (b) Rank abundance curve of the detected molecular formulae, and (c) Cumulative rank abundance curve. Molecular formulae are colour-coded by the percentage of samples in which they were detected.

Third, thousands of molecular formulae may be grouped based on their molecular properties into a much smaller number of compound classes. When grouped into seven compound classes based on the elements they contain, the relative abundance of these classes was very different (Fig. 3). The most dominant class (CHO)

was almost three orders of magnitude more abundant than the least abundant class (CHOSP) (Fig. 3). Differences between the lake types were also apparent (Fig. 3). The summation of parts with similar properties for dimensional reduction is referred to as *amalgamation* in CoDa analysis (Egozcue and Pawlowsky-Glahn, 2005; Quinn and Erb, 2020). Through amalgamation, the interpretation of the high-dimensional data becomes more manageable, and zeros can disappear if any one of the parts has a non-zero value. However, the amalgamation of parts will inevitably lead to the loss of information about the individual influence of the amalgamated parts and their relationships.

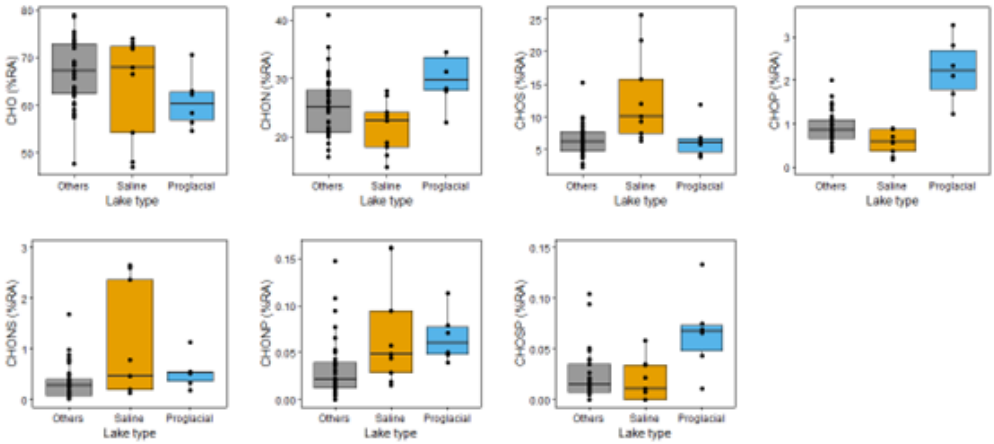

Figure 3: **Distributions of compound classes depending on lake types.** The horizontal lines of the boxes represent the first, second (median), and third quartiles. %RA = per cent relative abundance.

In the following sections, we analyse the relative abundance of mass peaks using both standard and CoDa methods. The analysis of summarised compound classes is provided in the Supplementary Discussion 2.1 and 2.2 for parsimony. Importantly, whether these two approaches yield similar or divergent results remains unknown until a direct comparison is conducted, which is seldom undertaken and is, in any case, problematic, as the two approaches are based on different assumptions. In particular, the assumptions concerning the sample space are critical. As basic examples, we will examine correlation or network analysis and regression analysis for R analysis and principal component analysis (PCA) for Q analysis, respectively.

3.2 Association of peak intensities

Proportionality analysis is increasingly recognised as a more appropriate measure of association than ordinary correlation analysis in CoDa, where variance

rather than absolute Euclidean distance should be used to quantify relationships (Aitchison et al., 2002; Lovell et al., 2015) (Fig. 1). Correlation analysis among peak intensities is commonly employed to assess associations; however, it has been criticised in gene sequence data analysis that has very similar data structures (Friedman and Alm, 2012; Skinnider et al., 2019; Kurtz et al., 2015; Gloor et al., 2017).

Proportionality, related to the variance of the logratios between variables, quantifies the extent to which two variables (x, y) maintain a constant ratio ($y = mx$ where m is a positive constant). Several proportionality indices have been proposed (Fig. 1), including ϕ (Lovell et al., 2015) and its symmetric analogue ρ (Erb and Notredame, 2016), both of which outperformed 15 other association measures in network reconstruction and clustering performance in transcriptomics, surpassing commonly used metrics such as Euclidean distance and Pearson or Spearman correlations (Skinnider et al., 2019). Additionally, SparCC (Friedman and Alm, 2012) and SPIEC-EASI (Kurtz et al., 2015) have been proposed for handling left-censored, sparse datasets, such as 16S rRNA gene profiling. Given the structural similarity between 16S rRNA sequence data and FT-ICR MS data, discussions of associations and correlation networks between genes (Erb and Notredame, 2016; Friedman and Alm, 2012; Skinnider et al., 2019; Kurtz et al., 2015) are also relevant to FT-ICR MS data. The first application of SPIEC-EASI to FT-ICR MS relative intensities was reported in Fonvielle et al. (2021). Most recently, the proportionality index of parts (PIP) has been introduced (Egozcue and Pawlowsky-Glahn, 2023). PIP is defined as:

$$PIP(X_1, X_2) = \frac{1}{1 + \sqrt{\tau_{12}}}, \text{ with } \tau_{12} = Var(X_1/X_2) \tag{2}$$

, where $Var(X_1/X_2)$ is the entry of the variation matrix of observations. Unlike previous indices, PIP remains invariant to subcomposition selection, addressing a key limitation of existing proportionality measures. The first application of PIP to FT-ICR MS relative intensities was reported in Kida et al. (2025). Table 2 summarises the properties of association measures for CoDa based either on proportionality or correlation.

We examine how the compositional nature of the relative peak intensities of FT-ICR MS can interfere with their correlation analysis. Specifically, we demonstrate how subsetting peaks influences correlations among the relative intensities of the remaining peaks. Figure 4 illustrates differences in Spearman correlation coefficients among the relative intensities of common peaks in the exemplary dataset (Kida et al., 2023), comparing two normalisation approaches: one using the entire dataset (Full normalisation) and the other using only the subset of common peaks (Subset normalisation). Despite their smaller numbers, these common

Table 2: Summary of proportionality- or correlation-based association measures for compositional data. ρ_{symb} = symmetric balance, $\rho_{|R}$ = partial correlation.

Index	Range	Interpretation	Subcompositional coherence	Negative association	Reference
Proportionality					
ϕ	0 to ∞	perfect proportionality:0 (prop.)	No	Not allowed	(Lovell et al., 2015)
ρ	-1 to 1	reciprocality:-1, perfect prop.:1	No	Reciprocality[b]	(Erb and Notredame, 2016)
PIP	0 to 1	no prop.:0, perfect prop.:1	Yes	Not allowed	(Egozcue and Pawlowsky-Glahn, 2023)
Correlation					
ρ_{symb}	-1 to 1	Same as Pearson correlation[a]	No	Allowed[c]	(Kynčlová et al., 2017)
$\rho_{\|R}$	-1 to 1	Same as Pearson correlation[a]	No	Allowed[c]	(Erb, 2020)
SparCC	-1 to 1	Same as Pearson correlation[a]	No	Allowed[c]	(Friedman and Alm, 2012)

[a] However, it is not a correlation between the original components, but relative to the others.
[b] The interpretation of perfect reciprocality is difficult, and reciprocality is not subcompositionally coherent.
[c] However, a negative correlation can change dramatically and unexpectedly with the subcomposition considered.

peaks accounted for approximately 70% of the total intensities. Ideally, correlations among these common peaks should remain consistent irrespective of which peaks are included in the dataset. However, many peak pairs exhibited varying correlations depending on the specific peaks considered (deviation from the 1 : 1 line). In extreme cases, even the sign of correlation was reversed with similar absolute coefficient values (Fig. 4a). Comparing the density distributions, correlations tended to be more negative when only common peaks were considered (y-axis, subset normalisation) compared to when all peaks were considered (x-axis, full normalisation)(Fig 4a). As a result, the distribution of the differences in Spearman correlations (X-Y) was clearly skewed to positive values (Fig. 4b). These comparisons demonstrate that the relative intensities of mass peaks are not independent of one another and are influenced by peak selection (i.e., *subcompositionally incoherent*). In other words, the sum constraint cannot be ignored, even when analysing thousands of peaks. This result may be surprising given the recently proposed "robust" use of Spearman correlation for associations among peak intensities (Kew et al., 2024), highlighting the need to acknowledge the compositionality of FT-ICR MS data. It is worth noting that any method of correlation (Pearson, Spearman, Kendall, etc.) will suffer from the same problem (Egozcue and Pawlowsky-Glahn, 2023). Additionally, the selection of peaks for analysis depends on how contamination peaks and noise are removed from raw spectra. The absence of a standardised method for this removal raises significant concerns that warrant further investigation. Furthermore, the number of assigned molecular formulae *per se* can differ depending on the instrument and data processing software used (Hawkes et al., 2020). The observed subcompositional incoherence in relative peak intensities implies that even common peaks identified across different studies are not directly comparable unless the whole set of considered peaks

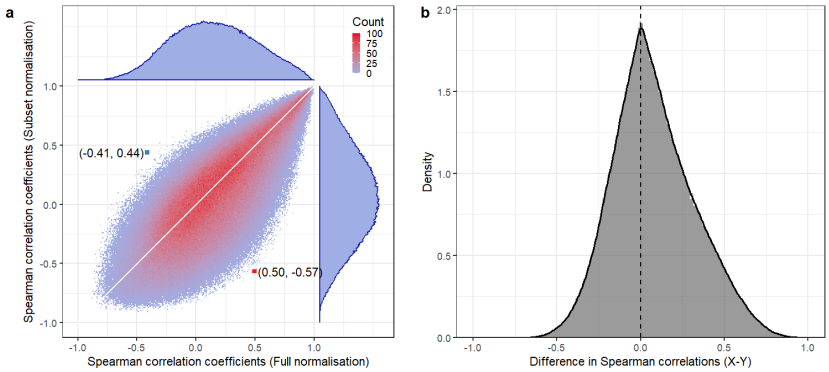

Figure 4: **The correlation of relative intensities is sensitive to the selection of mass peaks for analysis.** (a) A 2D histogram of the Spearman correlation coefficient observed for the relative intensities of common peaks ($n = 1214$) in the Antarctic lake dataset (48 samples) (Kida et al., 2023). The correlations were calculated in two ways: Full normalisation - intensities of all peaks detected ($n = 9910$) were first normalised per sample, and correlations were then computed among the subset of common peaks (x-axis). Subset normalisation - only the common peaks were considered, intensities were normalised within this subset per sample, and correlations were then computed (y-axis). Each point compares the correlation coefficient of the same sample pair between these two approaches. The offset from the 1:1 line shows that correlation values can shift depending on the normalisation procedure, indicating *subcompositional incoherence*. The extremes with the largest differences are annotated. Counts of correlation pairs (in total $\approx 0.74M$) are binned on a 250×250 grid. (b) Density plot of the differences between Spearman correlations (X-Y). A similar result was obtained for the Pearson correlation coefficient (not shown). The proportionality index PIP remains unchanged between the two cases (see manuscript).

is identical across datasets.

It is important to remember that the subcompositional incoherence also applies to the absolute mass peak intensities. There is recent progress in hyphenated (liquid chromatography) FT-ICR MS analysis, which enables direct analysis of NOM from natural water without prior solid-phase extraction (e.g., Lechtenfeld et al. (2024)). One may be tempted to consider the absolute peak intensities so collected as free of the mathematical sum constraint and thus free of compositional problems. However, as pointed out earlier, absolute abundance always has an upper limit constrained by the sample size or sampling design, and the absolute and the corresponding relative abundances essentially carry the same compositional information. Even where absolute intensities are recorded, ionization competition, space-charge and detector dynamics, and feature-calling (peak detection, feature extraction, operational blank subtraction, etc) thresholds impose an effective closure at the scan or chromatographic-segment level; logratio infer-

ence therefore remains appropriate unless linear response and constant recovery are demonstrated. Importantly, as chromatographic elution partitions the signal into subcompositions according to retention time, subcompositionally coherent methods such as logratios (or balances) within segments (or after an intensity-weighted aggregation of segments, if a single sample-level value is desired) are still the most robust basis for inference and for comparing solid phase extraction-based with non-extracted workflows. If hyphenated measurements verify linear response and stable recovery, conventional analyses may approximate CoDa analyses at the sample level (but not at the segment level). Nevertheless, logratios should remain the primary analysis, because they remain robust when those assumptions are not fully met.

We further investigated whether this subcompositional incoherence would affect the clustering of the common molecular formulae. Figure 5 shows the hierarchical clustering based on the distance matrix, computed as (1− Spearman correlation) among all possible pairs. We found that, despite the mathematical constraints, the hierarchical clustering performed reasonably in capturing overall associations between the common molecular formulae (Fig. 5a, b). In particular, the molecular properties of the assigned formulae in each corresponding cluster remained relatively constant, such as the dominance of nitrogen (N)-rich molecular formulae in CL2-5, as well as the positions of the molecular formulae on the van Krevelen diagrams (Fig. 5). Still, some significant differences were noticeable, such as the considerably different numbers of molecular formulae assigned in the corresponding clusters and the absence of N3-molecular formulae in CL2 in panel (b) (Fig. 5a, b). Furthermore, assignments of N-free molecular formulae were apparently switched between CL1 and CL3 in panels (a) and (b), making their associations with N-rich molecular formulae in CL3 uncertain (that is, it can easily change with the way normalisation is performed). Whether these differences are acceptable depends on the study question, and there is no guarantee that similar results can always be obtained.

These problems related to subcompositional incoherence can be effectively addressed by analysing the ratios of peak pairs (Fig. 1). The ratios remain constant regardless of the specific peaks considered in the dataset, with or without normalisation (i.e., *subcompositionally coherent*). Thus, univariate statistics on ratios can be validly compared across studies that share common peaks. The proportionality index PIP explicitly utilises ratios between parts (Egozcue and Pawlowsky-Glahn, 2023). In Fig. 5c, we provide the hierarchical clustering based on the PIP matrix, computed as (1− PIP) among all possible pairs. Compared to the clustering based on the Spearman correlation (Fig. 5a, b), PIP more clearly separated molecular formulae based on N content, albeit with similarity in overall clustering. Molecular formulae in CL1, CL4, and CL5 were N-free, and all molecular formulae with three N were assigned in CL2 (Fig. 5c).

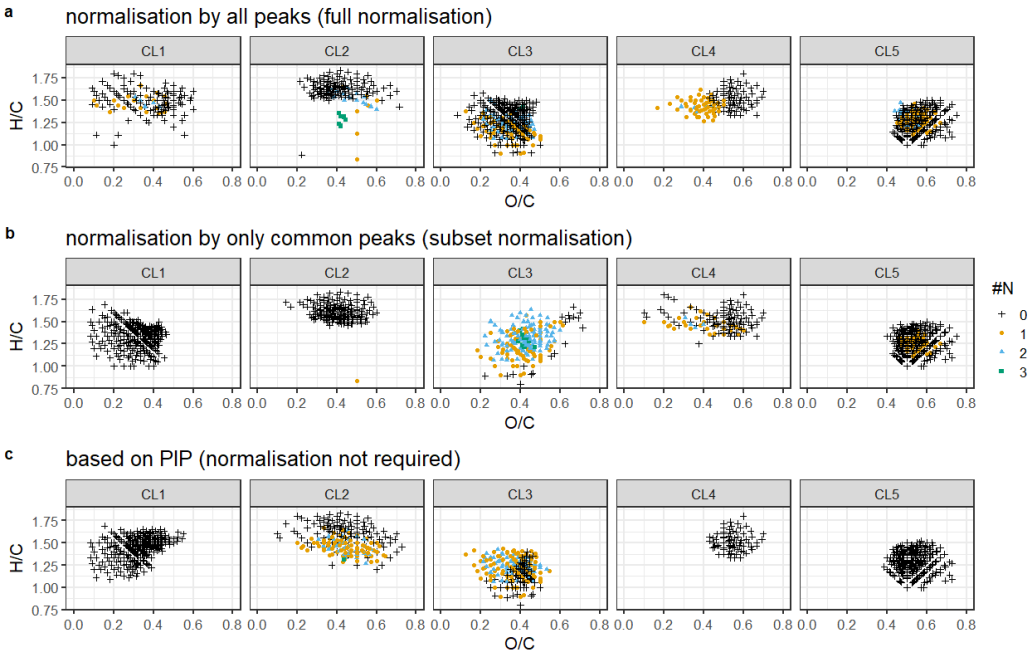

Figure 5: **Hierarchical clustering of common molecular formulae based on their Spearman correlations analysed in the two ways of peak intensity normalisation as in Fig. 4 (a, b) and that based on the proportionality index of parts (PIP) (c).** Panels show van Krevelen diagrams of the four molecular formulae clusters. The coloured symbols represent molecular formulae with different numbers of N atoms of the respective cluster. CL = cluster. The number of molecular formulae in each cluster are: CL1, 140; CL2, 143; CL3, 343; CL4, 132; and CL5, 254 in panel (a), CL1, 261; CL2, 175; CL3, 203; CL4, 145; and CL5, 242 in panel (b), and CL1, 261; CL2, 239; CL3, 225; CL4, 71; and CL5, 209 in panel (c). Agglomeration was based on the Ward linkage algorithm. The optimal number of clusters was decided by the silhouette value (Rousseeuw, 1987), where the number of clusters that maximised the average silhouette value of all molecular formulae was chosen. Molecular formulae with the silhouette value lower than 0 were excluded.

In some cases, the symmetric proportionality coefficient ρ can give similar results. The first application of ρ to FT-ICR MS relative intensities was reported by Osterholz et al. (2022) to infer dissolved organic matter-microbe networks. When zeros are present in the dataset, they must be properly handled before ratio calculation. In Osterholz et al. (2022), zeros were replaced with one-tenth of the minimum relative intensity across the dataset. These cases might happen when the subset of parts considered represents a large part of the total sum, implying that the renormalisation has little impact and is hardly noticeable. Nevertheless, further study is needed to establish rules on when this might happen and to determine if

other issues arise. The lack of subcompositional coherence of ρ indicates that it might be difficult to control.

As another demonstration, we present a network of common molecular formulae from the exemplary Antarctic lake dataset (Kida et al., 2023), constructed using PIP (Fig. 6) or ρ (Fig. S5) and visualised using the open-source software Gephi (Bastian et al., 2009). Neighbouring molecular formulae directly linked by

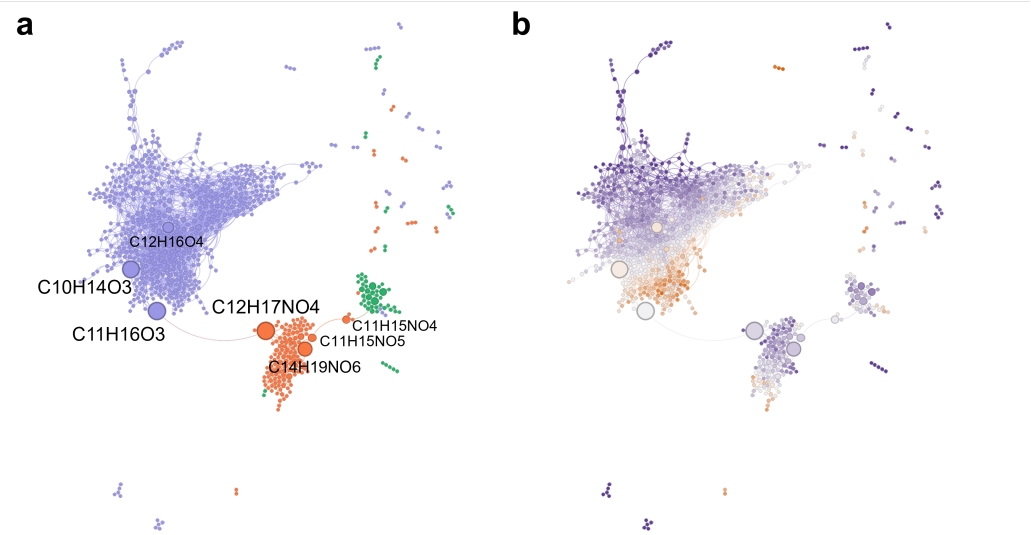

Figure 6: **Network analysis of the common peaks of the exemplary Antarctic lake dataset** (Kida et al., 2023) **based on the proportionality index of parts (PIP)**. Only peak pairs with PIP values > 0.90 were selected, resulting in 838 peaks (out of the 1214 common peaks) and 8088 pairs. Peaks are represented by points (nodes), and highly proportional pairs are linked by non-directional lines (edges). In (a), nodes are colour-coded based on the N content: blue $= 0$, orange $= 1$, and green $= 2$, while in (b), colour code is based on the modified aromaticity index (Koch and Dittmar, 2006), with red colours indicating higher values. The node size is proportional to the betweenness centrality metric. Molecular formulae of the key nodes acting as the "hub" are labelled. The network layout algorithm was by ForceAtlas2 (Jacomy et al., 2014). Nodes with a single edge (leaves) were removed for parsimony.

lines (edges) can be viewed as exhibiting highly co-varied behaviour across the dataset, likely driven by shared biogeochemical processes. Notably, three distinct clusters of molecular formulae emerged, clearly separated by N atom content (Fig. 6a). Molecular formulae with the same N content thus co-varied more closely with each other than those with different N content, in line with the clustering result (Fig. 5c). Clusters with one more or one less N content were connected, implying continuous DOM transformation processes with N additions or losses. In

these continuous DOM transformation processes, certain "key" molecular formulae served as bridges between and within clusters (Fig. 6a). Additionally, within each cluster, molecular formulae exhibited tighter associations based on molecular properties, exemplified by the modified aromaticity index (Koch and Dittmar, 2006) (Fig. 6b). Similar results were obtained in this case when the network was constructed based on ρ (Fig. S5). Interestingly, sulfur-containing molecular formulae formed a separate cluster (Fig. S5), indicating distinct processes governing their relative abundance. These processes likely involve abiotic sulfurization in stratified, hypersaline lakes, a phenomenon uncommon in the other lakes (Kida et al., 2023). Beyond molecular clustering and networking, these proportionality indices can also be used for other purposes, such as ordination and multivariate comparisons. Furthermore, this network analysis approach can be extended to integrate additional datasets, such as microbial community composition, as was done previously (Osterholz et al., 2022; Kida et al., 2025).

3.3 Regression analysis and statistical inference

Regression analysis is an R analysis to quantitatively assess relationships between a dependent variable (response) and one or more independent variables (covariates). When CoDa is involved, there are three types of regression: regression with compositional response, regression with compositional covariates, and regression with response and covariates both compositional (Morais and Thomas-Agnan, 2021). Using the first example, we will briefly explain how compositional regressions can be performed. When the response is compositional, residuals should be computed within the framework of the Aitchison geometry of the simplex and not within the framework of the usual Euclidean geometry in real space, as the Euclidean distance loses meaning for CoDa. When the covariates are compositional, the classical least-squares fitting may be applied using the Euclidean geometry for the residuals, but the covariates must be expressed in logratio coordinates (specifically, ilr). Transformation from compositional vectors to logratio vectors using alr, clr, or ilr transformation results in multivariate linear modeling with the assumed normality of the residuals (Egozcue et al., 2012; Pawlowsky-Glahn et al., 2015; Aitchison, 2005), which can be proceeded with in a standard way, with standard unconstrained multivariate tests and the usual forms of residual analysis. For the last case where response and covariates are both compositional, the straightforward approach consists of taking coordinates separately for each of the two sets of samples and proceeding as usual in multiple, multivariate regressions.

In the first example of regression with compositional response, we estimate the relative abundance of compound classes in the Antarctic lake dataset (Kida et al., 2023) by environmental variables using a generalized additive model for location, scale and shape (GAMLSS) (Rigby and Stasinopoulos, 2005). Envi-

ronmental variables such as water pH and electrical conductivity (EC) affect the chemical diversity of DOM in these lakes (Kida et al., 2023), thus they were used as covariates in the regression (Fig. 7). The composition was first represented

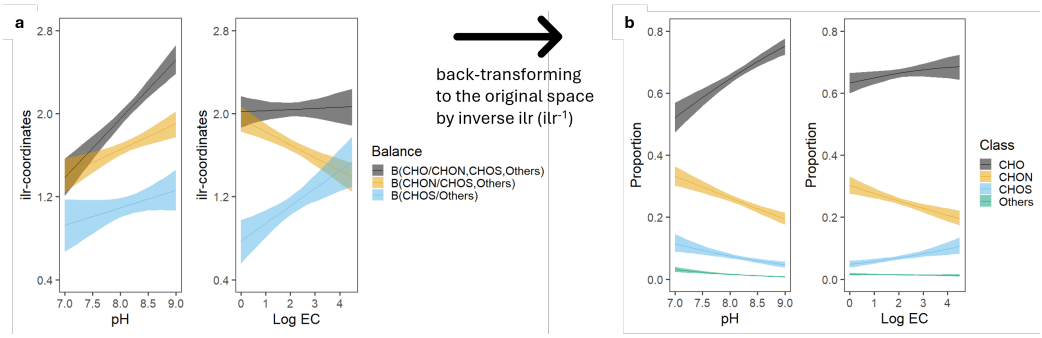

Figure 7: **Marginal effects of environmental variables (pH and log EC) on the relative abundance of compound classes of the exemplary Antarctic lake dataset** (Kida et al., 2023)**, by GAMLSS analysis**. Minor compound classes (CHOP, CHONS, CHONP, and CHOSP) were amalgamated as Others for parsimony. Regression analyses were first conducted in the ilr-coordinates (balances) constructed by sequential binary partitioning (a), then the results were back-transformed by inverse ilr and depicted in the original compositional space (b). The shaded areas represent 95% confidence intervals. The 95% CIs in the original compositional space were derived from 1000 simulations of the regression model in the ilr coordinates. Predicted means from each simulation were back-transformed to the original compositional space, and the lower and upper bounds of the intervals were defined as the $2.5th$ and $97.5th$ percentiles of these back-transformed predictions.

in the ilr-coordinates using sequential binary partitioning (SBP) (Egozcue and Pawlowsky-Glahn, 2005), representing meaningful geochemical processes (Fig. 7a). Here, an increase in the first balance, B(CHO/CHON,CHOS,Others), represents all processes retaining CHO-only molecular formulae, an increase in the second balance, B(CHON/CHOS,Others), is related to fresh, N-rich DOM abundant in proglacial lakes, and an increase in the third balance, B(CHOS/Others), is indicative of abiotic sulfurization in saline lakes (Kida et al., 2023). The covariates had a contrasting influence on the first and second balances, that is, pH tended to increase while EC decreased or had little effect on them (Fig. 7a). The third balance, contrarily, tended to increase with both pH and EC. The trends in the increase/decrease of CHO, CHON, and CHOS classes with respect to other compound classes along environmental gradients agreed with the observed patterns that were largely explained by the dominance of N-rich DOM in proglacial lakes and S-rich DOM in saline lakes (Kida et al., 2023).

The simplicial regression in the ilr-coordinates fully complies with the Aitchison geometry and is a valid analysis for CoDa, while further back-transforming

the result in the original compositional space by the inverse ilr transformation (ilr^{-1}) may help understand the result more intuitively. The predicted trends in the relative abundance of each compound class along pH or EC are shown in Fig. 7b. However in our case, the increase in the relative abundance in CHO class decreased that of the other classes due to the sum constraint. The balances (relative increase/decrease) among other classes were not clear on the relative scale (especially along pH) and could only be explicitly analysed using ilr-coordinates (Fig. 7). We note that, due to the distortion of the geometry when mapping points from ilr-coordinates (the real space) to the compositional space (simplex), confidence intervals (CIs) can not be correctly mapped by the inverse ilr transformation. To overcome this problem, we took the following approach: First, we performed 1000 random draws from a multivariate normal distribution with a mean vector equal to the estimated model coefficients and a covariance matrix equal to the covariance matrix of the coefficients. Then, we obtained random predictions (means) for each ilr-coordinate, which were back-transformed to the compositional scale by the inverse ilr transformation. Finally, we calculated the quantiles (2.5% and 97.5%) of the back-transformed predictions for the classical 95% CIs. This approach should work for any regression analysis with a compositional response, thus providing sound means for statistical inference of regression analyses of CoDa.

3.4 PCA of peak intensities

Ordination techniques are frequently used in Q analysis to summarize and visualize multidimensional information in a lower-dimensional space. Principal component analysis (PCA) is the most suitable method for exploratory ordination analysis of CoDa, as logratio variance is the proper measure of the distance between parts (Gloor et al., 2017; Isles, 2020) (Fig. 1). PCA of CoDa (sometimes referred to as CoDa-PCA) theoretically offers several advantages over principal coordinate analysis (PCoA) based on a dissimilarity matrix computed from relative abundances. These advantages include greater stability for data subsetting and improved reproducibility, thanks to the use of the Aitchison distance as input (Gloor et al., 2017). Since PCA is a multidimensional extension of correlation analysis, issues inherent to correlation analysis of CoDa also apply to PCA. The solution for this is simple – apply a clr transformation to the relative data before performing PCA. This approach measures the distance between samples using the Aitchison distance. The first application of CoDa-PCA to compound classes or relative peak intensities of NOM measured by FT-ICR MS was reported by Kida et al. (021a) and Fonvielle et al. (2021), respectively.

When analyzing FT-ICR MS relative peak intensities, the prevalence of numerous zeros in the dataset hampers the clr-transformation required for CoDa-

PCA. In their study, Fonvielle et al. (2021) addressed this challenge by imputing zeros with small values based on a Bayesian-multiplicative replacement approach using the *zCompositions* R package (Palarea-Albaladejo and Martín-Fernández, 2015), which was not explicitly detailed in their paper but can be found in their supplementary R code (their Supporting Information S2). Alternatively, another approach involves a simple replacement of zeros with a value smaller than the detection limit, as was done in Osterholz et al. (2022). In any case, the choice of zero handling method requires careful consideration, as it can introduce unwanted distortion in feature relationships (Lubbe et al., 2021; Martín-Fernández et al., 2011).

In Figure 8a-c, we compare ordinary PCA and CoDa-PCA applied to FT-ICR MS relative intensities using the exemplary Antarctic dataset (Kida et al., 2023). For CoDa-PCA, clr transformation was conducted in two different ways: the first was robust clr (rclr) transformation of peak intensities, where the geometric mean was calculated only from non-zero peak intensities (Martino et al., 2019) (equation (4) in Supplementary Information). In high-dimensional data, the geometric mean of rclr approximates the true geometric mean of clr (Martín-Fernández et al., 2015). The second method involved applying the clr transformation after replacing zeros with $1/100$th of the smallest relative intensity across the dataset. For R users, both clr and rclr transformations have been integrated into the popular *vegan* package (Oksanen et al., 2024) since version 2.6-4. Furthermore, we compare these PCA results with PCoA based on Bray-Curtis dissimilarity and Jensen-Shannon distance computed from FT-ICR MS relative intensities (Figure 8d,e) because PCoA is the most common, non-compositional ordination method that has been preferred in NOM research.

The results of the ordinations were largely consistent across these methods. The ordinary PCA and CoDa-PCA after rclr transformation were similar, with CoDa-PCA after rclr transformation explaining slightly more variation (Fig. 8a,b). In both ordinary PCA and CoDa-PCA after rclr transformation, sample distributions aligned well with the predetermined clustering (Fig. 8a,b). In contrast, CoDa-PCA with clr transformation following zero imputation resulted in less clear sample differences and the lowest explained variation (Fig. 8c). Similar results were obtained by zero imputations with $1/10$th or $1/1000$th of the smallest value (not shown). Some freshwater lakes were placed near a hypersaline lake (CL4), while another hypersaline lake (CL3) was placed alongside the CL2 freshwater lake cluster (Fig. 8c). These results suggest that zero imputations with a small value obscured sample distinctions because numerous identical imputed values were introduced across samples. At the same time, the PCoA approaches captured similar structures at the sample level with those of the ordinary PCA and CoDa-PCA after rclr transformation (note that the explained variation in CoDa-PCA and PCoA is not comparable because they are defined in different spaces)

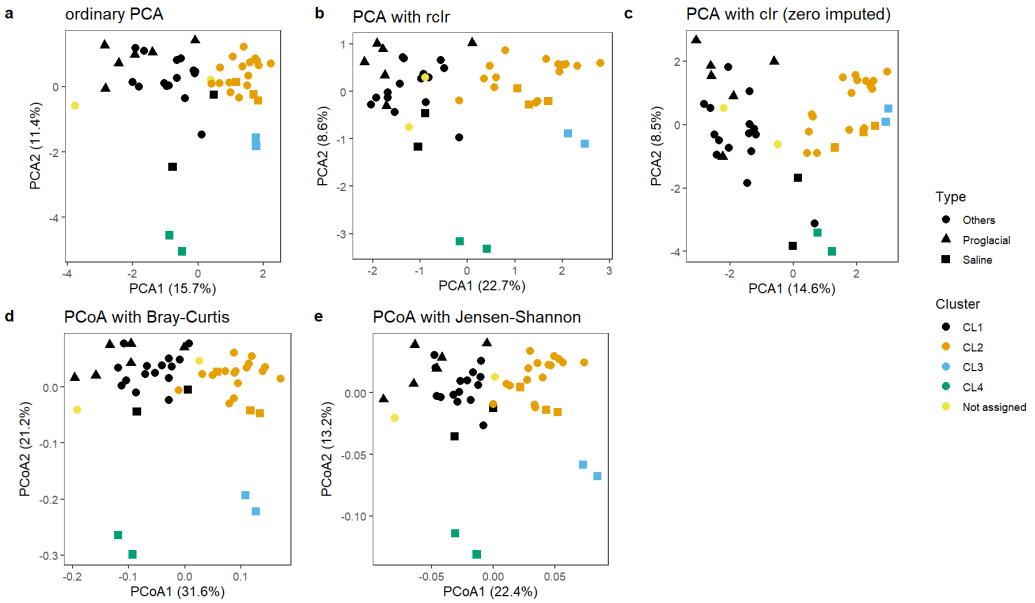

Figure 8: **Comparison of principal component analysis (PCA) of the original (a), robust** clr**-transformed (b), and** clr**-transformed (c) FT-ICR MS relative intensities, and principal coordinate analysis (PCoA) based on Bray-Curtis dissimilarity (d) and Jensen-Shannon distance (e) computed from relative intensities.** To provide a reference, samples were colour-coded based on predetermined clusters derived from the frequency distributions of the double-bond equivalent of molecular formulae across samples (Kida et al., 2023), which excluded the peak intensity information to avoid compositional problems (Please note that this cluster is different from that in Fig. 5). In (c), zeros were replaced with 1/100th of the smallest relative intensity across the dataset prior to clr transformation. The mode of PCA plots is distance (scaling 1) (Legendre and Legendre, 2012b) or form (Aitchison and Greenacre, 2002) plots, where distances between samples are preserved as much as possible, up to the projection. We want to stress here that any ordination plot must always be plotted with the "aspect ratio" of 1:1, ensuring that one unit on the x-axis is the same length as one unit on the y-axis, so that distances between samples ("sites", in scaling 1) or relationships ($\cos\theta$) between variables ("species", in scaling 2) remain preserved. Any arbitrary elongation or shortening of either axis to fit the plot in the page space will distort relationships between samples or variables.

(Fig. 8d,e). The PCoA based on Bray-Curtis dissimilarity may have worked well for this particular case because the Bray-Curtis dissimilarity ignores "double zeros" and is not affected by the presence of many zeros (Zuur et al., 2010). These findings suggest that, at least for the exemplary dataset, ignoring compositionality does not always result in distorted sample-level patterns. In other words, for the ordination analysis of FT-ICR MS relative intensities, there are cases where approximations based on non-compositional methods can still capture the ma-

jor trends among samples. This is encouraging for researchers who have so far used conventional PCA or PCoA in previous studies, as their major conclusions at the level of sample ordination may remain valid despite not having explicitly accounted for compositionality. Nevertheless, as you never know in advance if approximations give reasonable results from a statistical point of view, it would be wise to recheck the data using compositionally compliant methods.

We note that such robustness of non-compositional methods is resolution-dependent. While ordination methods focusing on relationships among samples can tolerate approximations, analyses at finer resolution, such as associations among individual molecular formulae, or between molecular formulae and microbial taxa, require strict consideration of compositionality. As shown in Fig. 4 and Fig. 5, ignoring compositional constraints in R-mode analyses leads to subcompositional incoherence and spurious associations. Thus, while non-compositional ordination may be acceptable as an approximation at the sample level, rigorous compositional methods remain indispensable for molecular- and network-level analyses. Even for ordination methods in future applications, it is advisable to use compositional methods grounded on sound mathematical principles for CoDa. Another possible alternative for calculating the dissimilarity matrix may be using the presence-absence data of mass peaks (i.e., Jaccard distance), albeit with a loss of abundance information.

4 Concluding remarks and future directions

In this tutorial paper, we discussed the application of compositional data (CoDa) analysis in natural organic matter research using FT-ICR MS data as an example. Importantly, this approach can be extended to virtually all analytical instruments that produce signal or peak intensities that are analysed in relative scale, such as fluorescence spectroscopy and NMR. Microbiologists have already adopted CoDa methods to microbial composition data by high-throughput sequencing (Gloor et al., 2017), which is now frequently combined with organic matter data. It is crucial to always consider the sample space of the data before conducting any statistical analysis; ordinary statistical methods developed for real random data may yield misleading and spurious results if applied to CoDa. Compositional data are ubiquitous in environmental research, and we firmly anticipate their applications to grow significantly in the future (Fig. 1).

The core concept of CoDa analysis involves using (log)ratios between variables. This ensures the fundamental principle of subcompositional coherence (Aitchison and Egozcue, 2005) in compositional (relative) data, where relationships between parts remain consistent, regardless of the other parts considered in the dataset. This paper focuses on the practical aspects of working with FT-ICR MS data. Interested readers are referred to other papers and books that deal with the theories and wider applications of CoDa methods in various fields and analytical techniques, which are listed in the Appendix.

Conflict of Interest Statement

The authors declare that the research was conducted in the absence of any commercial or financial relationships that could be construed as a potential conflict of interest.

Author Contributions

CRediT roles: MK: Conceptualization, Formal analysis, Funding acquisition, Methodology, Project administration, Resources, Software, Visualization, Writing - original draft; JM: Formal analysis, Methodology, Software; TD: Writing - review and editing; JJE and VPG: Formal analysis, Funding acquisition, Methodology, Software, Validation; all authors: Writing - review and editing.

Funding

This work was supported by JSPS KAKENHI 22H03733/23K24987 and JST FOREST (Fusion Oriented REsearch for disruptive Science and Technology) Program JPMJFR231C (MK). MK was also partially supported by startup funding from Kobe University. JJE and VPG were supported by the grants PID2021-123833OB-I00 and PID2021-123833OB-I00, funded by the Spanish Ministry of Science, Innovation and Universities (MICIU/AEI/10.13039/501100011033/) and "ERDF A way of making Europe".

Acknowledgments

We thank Helena Osterholz for initial discussions. Figure 4a was created using the R code from Lovell et al. (2015). Figure S3 and Figure S4 were created using the R code from Greenacre et al. (2021). The R code and supplementary data to reproduce other figures (including those in Supplementary Information) are available at figshare (https://doi.org/10.6084/m9.figshare.30344623.v2).

References

Abdi, D., B. J. Cade-Menun, N. Ziadi, and L.-É. Parent (2015). Compositional statistical analysis of soil 31p-nmr forms. *Geoderma 257*, 40–47.

Aitchison, J. (1982). The statistical analysis of compositional data (with discussion). *Journal of the Royal Statistical Society, Series B (Statistical Methodology) 44*(2), 139–177.

Aitchison, J. (1983). Principal component analysis of compositional data. *Biometrika 70*(1), 57–65.

Aitchison, J. (1984). Reducing the dimensionality of compositional data sets. *Mathematical Geology 16*(6), 617–636.

Aitchison, J. (1986). *The Statistical Analysis of Compositional Data*. Monographs on Statistics and Applied Probability. London (UK): Chapman & Hall Ltd., London (UK). (Reprinted in 2003 with additional material by The Blackburn Press). 416 p.

Aitchison, J. (1992). On criteria for measures of compositional difference. *Mathematical Geology 24*(4).

Aitchison, J. (2005). A concise guide to compositional data analysis. Unpublished techreport, http://ima.udg.edu/Activitats/CoDaWork05/.

Aitchison, J. (2008). The single principle of compositional data analysis, continuing fallacies, confusions and misunderstandings and some suggested remedies. In J. Daunis-i Estadella and J. A. Martín-Fernández (Eds.), *Proceedings of CoDaWork'08, The 3rd Compositional Data Analysis Workshop*. http://dugi-doc.udg.edu/handle/10256/706.

Aitchison, J., C. Barceló-Vidal, J. J. Egozcue, and V. Pawlowsky-Glahn (2002). A concise guide for the algebraic-geometric structure of the simplex, the sample space for compositional data analysis. In *Proceedings of IAMG'02 – The VIII Annual Conference of the International Association for Mathematical Geology*, pp. 387–392.

Aitchison, J., C. Barceló-Vidal, J. A. Martín-Fernández, and V. Pawlowsky-Glahn (2000). Logratio analysis and compositional distance. *Mathematical Geology 32*(3), 271–275.

Aitchison, J. and J. J. Egozcue (2005). Compositional data analysis: where are we and where should we be heading? *Mathematical Geology 37*(7), 829–850.

Aitchison, J. and M. Greenacre (2002). Biplots for compositional data. *Journal of the Royal Statistical Society, Series C (Applied Statistics) 51*(4), 375–392.

Arts, M. T., R. D. Robarts, F. Kasai, M. J. Waiser, V. P. Tumber, A. J. Plante, H. Rai, and H. J. de Lange (2000). The attenuation of ultraviolet radiation in high dissolved organic carbon waters of wetlands and lakes on the northern great plains. *Limnology and Oceanography 45*(2), 292–299.

Bahureksa, W., M. M. Tfaily, R. M. Boiteau, R. B. Young, M. N. Logan, A. M. McKenna, and T. Borch (2021). Soil organic matter characterization by fourier transform ion cyclotron resonance mass spectrometry (fticr ms): A critical review of sample preparation, analysis, and data interpretation. *Environmental Science & Technology 55*(14), 9637–9656.

Baldock, J., J. Oades, P. Nelson, T. Skene, A. Golchin, and P. Clarke (1997). Assessing the extent of decomposition of natural organic materials using solid-state 13c nmr spectroscopy. *Soil Research 35*(5), 1061–1084.

Barceló-Vidal, C. and J.-A. Martín-Fernández (2016). The mathematics of compositional analysis. *Austrian Journal of Statistics 45*, 57–71.

Bastian, M., S. Heymann, and M. Jacomy (2009). Gephi: an open source software for exploring and manipulating networks. In *Proceedings of the international AAAI conference on web and social media*, Volume 3, pp. 361–362.

Bian, G., G. B. Gloor, A. Gong, C. Jia, W. Zhang, J. Hu, H. Zhang, Y. Zhang, Z. Zhou, J. Zhang, et al. (2017). The gut microbiota of healthy aged chinese is similar to that of the healthy young. *Msphere 2*(5), 10–1128.

Boogaart, K. G. v. and R. Tolosana-Delgado (2008). "compositions": a unified R package to analyze compositional data. *Computers & Geosciences 34*(4), 320–338.

Boogaart, K. G. v. and R. Tolosana-Delgado (2013). *Analyzing Compositional Data with R*. Use R! Springer Berlin, Heidelberg.

Chadwick, O. A. and J. Chorover (2001). The chemistry of pedogenic thresholds. *Geoderma 100*(3-4), 321–353.

Chayes, F. (1960). On correlation between variables of constant sum. *Journal of Geophysical Research (1896-1977) 65*(12), 4185–4193.

Coenders, G., J. J. Egozcue, K. Fačevicová, J. Navarro-López, C.and Palarea-Albaladejo, and R. Pawlowsky-Glahn, V. ans Tolosana-Delgado (2023). 40 years after Aitchison's article "the statistical analysis of compositional data". where we are and where we are heading. *SORT 47*(2), 207–228.

Dumuid, D., Ž. Pedišić, J. Palarea-Albaladejo, J. A. Martín-Fernández, K. Hron, and T. Olds (2020). Compositional data analysis in time-use epidemiology: what, why, how. *International journal of environmental research and public health 17*(7), 2220.

Egozcue, J. J., J. Daunis-i-Estadella, V. Pawlowsky-Glahn, K. Hron, and P. Filzmoser (2012). Simplicial regression. The Normal model. *Journal of Applied Probability and Statistics (JAPS) 6*(1–2), 87–108.

Egozcue, J. J., C. Gozzi, A. Buccianti, and V. Pawlowsky-Glahn (2024). Exploring geochemical data using compositional techniques: A practical guide. *Journal of Geochemical Exploration 258*, 107385.

Egozcue, J. J. and V. Pawlowsky-Glahn (2005). Groups of parts and their balances in compositional data analysis. *Mathematical Geology 37*(7), 795–828.

Egozcue, J. J. and V. Pawlowsky-Glahn (2018). Modelling compositional data. the sample space approach. In B. S. Daya Sagar, Q. Cheng, and F. Agterberg (Eds.),

Handbook of Mathematical Geosciences – Fifty Years of IAMG, pp. XXV, 875. Springer International Publishing.

Egozcue, J. J. and V. Pawlowsky-Glahn (2019). Compositional data: the sample space and its structure. *TEST 28*(3), 599–638.

Egozcue, J. J. and V. Pawlowsky-Glahn (2023). Subcompositional coherence and a novel proportionality index of parts. *SORT 47*(2), 229–244.

Egozcue, J. J., V. Pawlowsky-Glahn, and G. B. Gloor (2018). Linear association in compositional data analysis. *Austrian Journal of Statistics 47*(1), 3–31.

Egozcue, J. J., V. Pawlowsky-Glahn, G. Mateu-Figueras, and C. Barcelo-Vidal (2003). Isometric logratio transformations for compositional data analysis. *Math. Geol. 35*, 279–300.

Erb, I. and C. Notredame (2016). How should we measure proportionality on relative gene expression data? *Theory in Biosciences 135*(1-2), 21–36.

Erb, J. (2020). Partial correlations in compositional data analysis. *Applied Computing and Geosciences 6*, 9p.

Fernandes, A. D., J. N. Reid, J. M. Macklaim, T. A. McMurrough, D. R. Edgell, and G. B. Gloor (2014). Unifying the analysis of high-throughput sequencing datasets: characterizing RNA-seq, 16S rRNA gene sequencing and selective growth experiments by compositional data analysis. *Microbiome 2*, 15.1–15.13.

Filzmoser, P., K. Hron, and C. Reimann (2009). Univariate statistical analysis of environmental (compositional) data: Problems and possibilities. *Sci. Total Environ 407*, 6100–6108.

Filzmoser, P., K. Hron, and C. Reimann (2010). The bivariate statistical analysis of environmental (compositional) data. *Science of The Total Environment 408*(19), 4230–4238.

Filzmoser, P., K. Hron, and M. Templ (2018). *Applied Compositional Data Analysis – With Worked Examples in R*. Springer Series in Statistics. Springer Cham.

Fonvielle, J. A., D. P. Giling, T. Dittmar, S. A. Berger, J. C. Nejstgaard, A. Lyche Solheim, M. O. Gessner, H.-P. Grossart, and G. Singer (2021). Exploring the suitability of ecosystem metabolomes to assess imprints of brownification and nutrient enrichment on lakes. *Journal of Geophysical Research: Biogeosciences 126*(5), e2020JG005903.

Frerebeau, N. and A. Philippe (2025, January). nexus: Sourcing archaeological materials by chemical composition.

Friedman, J. and E. J. Alm (2012). Inferring correlation networks from genomic survey data. *PLoS Computational Biology 8*(9), e1002687.

Gloor, G. B. (2023, July). amIcompositional: Simple tests for compositional behaviour of high throughput data with common transformations. *Austrian Journal of Statistics 52*(4), 180–197.

Gloor, G. B., J. M. Macklaim, V. Pawlowsky-Glahn, and J. J. Egozcue (2017). Microbiome datasets are compositional: and this is not optional. *Frontiers Microbiology 8*, 2224.

Gloor, G. B. and G. Reid (2016). Compositional analysis: a valid approach to analyze microbiome high-throughput sequencing data. *Canadian journal of microbiology 62*(8), 692–703.

Graeve, M. and M. J. Greenacre (2020). The selection and analysis of fatty acid ratios: a new approach for the univariate and multivariate analysis of fatty acid trophic markers in marine pelagic organisms. *Limnology and Oceanography: Methods 18*(5), 196–210.

Greenacre, M. (2021). Compositional data analysis. *Annual Review of Statistics and Its Application 8*(Volume 8, 2021), 271–299.

Greenacre, M., M. Martínez-Álvaro, and A. Blasco (2021). Compositional data analysis of microbiome and any-omics datasets: a validation of the additive logratio transformation. *Frontiers in microbiology 12*, 727398.

Gupta, N., S. E. Mathiassen, G. Mateu-Figueras, M. Heiden, D. M. Hallman, M. B. Jørgensen, and A. Holtermann (2018). A comparison of standard and compositional data analysis in studies addressing group differences in sedentary behavior and physical activity. *International Journal of Behavioral Nutrition and Physical Activity 15*, 1–12.

Hawkes, J. A., J. d'Andrilli, J. N. Agar, M. P. Barrow, S. M. Berg, N. Catalán, H. Chen, R. K. Chu, R. B. Cole, T. Dittmar, et al. (2020). An international laboratory comparison of dissolved organic matter composition by high resolution mass spectrometry: Are we getting the same answer? *Limnology and Oceanography: Methods 18*(6), 235–258.

Hedges, J. I., R. G. Keil, and R. Benner (1997). What happens to terrestrial organic matter in the ocean? *Organic geochemistry 27*(5-6), 195–212.

Hertkorn, N., M. Harir, B. P. Koch, B. Michalke, and P. Schmitt-Kopplin (2013). High-field nmr spectroscopy and fticr mass spectrometry: powerful discovery tools for the molecular level characterization of marine dissolved organic matter. *Biogeosciences 10*(3), 1583–1624.

Hron, K., M. Templ, and P. Filzmoser (2010). Imputation of missing values for compositional data using classical and robust methods. *Computational Statistics and Data Analysis 54*(12), 3095–3107.

Hu, A., M. Choi, A. J. Tanentzap, J. Liu, K.-S. Jang, J. T. Lennon, Y. Liu, J. Soininen, X. Lu, Y. Zhang, et al. (2022). Ecological networks of dissolved organic matter and microorganisms under global change. *Nature communications 13*(1), 3600.

Isles, P. D. (2020). The misuse of ratios in ecological stoichiometry. *Ecology 101*(11), e03153.

Jacomy, M., T. Venturini, S. Heymann, and M. Bastian (2014). Forceatlas2, a continuous graph layout algorithm for handy network visualization designed for the gephi software. *PloS one 9*(6), e98679.

Kellerman, A. M., T. Dittmar, D. N. Kothawala, and L. J. Tranvik (2014). Chemodiversity of dissolved organic matter in lakes driven by climate and hydrology. *Nature communications 5*(1), 3804.

Kew, W., A. Myers-Pigg, C. H. Chang, S. M. Colby, J. Eder, M. M. Tfaily, J. Hawkes, R. K. Chu, and J. C. Stegen (2024). Reviews and syntheses: Opportunities for robust use of peak intensities from high-resolution mass spectrometry in organic matter studies. *Biogeosciences 21*(20), 4665–4679.

Kida, M., N. Fujitake, T. Kojima, Y. Tanabe, K. Hayashi, S. Kudoh, and T. Dittmar (2021a). Dissolved organic matter processing in pristine antarctic streams. *Environmental Science & Technology 55*(14), 10175–10185.

Kida, M., J. Merder, N. Fujitake, Y. Tanabe, K. Hayashi, S. Kudoh, and T. Dittmar (2023). Determinants of microbial-derived dissolved organic matter diversity in antarctic lakes. *Environmental Science & Technology 57*(13), 5464–5473.

Kida, M., A. Ohira, Y. Okazaki, Y. T. Yamaguchi, A. S. Goto, K. Hayakawa, and H. Nishimura (2025). Couples in the deep: dissolved organic and microbial communities in the oxygenated hypolimnion of a deep freshwater lake. *bioRxiv*, 2025–09.

Kida, M., I. Watanabe, K. Kinjo, M. Kondo, S. Yoshitake, M. Tomotsune, Y. Iimura, S. Umnouysin, V. Suchewaboripont, S. Poungparn, et al. (2021b). Organic carbon stock and composition in 3.5-m core mangrove soils (trat, thailand). *Science of the Total Environment 801*, 149682.

Koch, B. P. and T. Dittmar (2006). From mass to structure: An aromaticity index for high-resolution mass data of natural organic matter. *Rapid communications in mass spectrometry 20*(5), 926–932.

Koch, B. P., M. Witt, R. Engbrodt, T. Dittmar, and G. Kattner (2005). Molecular formulae of marine and terrigenous dissolved organic matter detected by electrospray ionization fourier transform ion cyclotron resonance mass spectrometry. *Geochimica et Cosmochimica Acta 69*(13), 3299–3308.

Konermann, L., E. Ahadi, A. D. Rodriguez, and S. Vahidi (2013). Unraveling the mechanism of electrospray ionization.

Kujawinski, E. B., P. G. Hatcher, and M. A. Freitas (2002). High-resolution fourier transform ion cyclotron resonance mass spectrometry of humic and fulvic acids: improvements and comparisons. *Analytical chemistry 74*(2), 413–419.

Kurtz, Z. D., C. L. Müller, E. R. Miraldi, D. R. Littman, M. J. Blaser, and R. A. Bonneau (2015). Sparse and compositionally robust inference of microbial ecological networks. *PLoS computational biology 11*(5), e1004226.

Kynčlová, P., K. Hron, and P. Filzmoser (2017). Correlation between compositional parts based on symmetric balances. *Mathematical Geosciences 49*, 777–796.

Lechtenfeld, O. J., J. Kaesler, E. K. Jennings, and B. P. Koch (2024). Direct analysis of marine dissolved organic matter using lc-ft-icr ms. *Environmental Science & Technology 58*(10), 4637–4647.

Legendre, P. and L. Legendre (2012a). Chapter 7 - ecological resemblance. In P. Legendre and L. Legendre (Eds.), *Numerical Ecology*, Volume 24 of *Developments in Environmental Modelling*, pp. 265–335. Elsevier.

Legendre, P. and L. Legendre (2012b). Chapter 9 - ordination in reduced space. In P. Legendre and L. Legendre (Eds.), *Numerical Ecology*, Volume 24 of *Developments in Environmental Modelling*, pp. 425–520. Elsevier.

Lovell, D., V. Pawlowsky-Glahn, J. J. Egozcue, S. Marguerat, and J. Bähler (2015, 03). Proportionality: A valid alternative to correlation for relative data. *PLoS Comput Biol 11*(3), e1004075.

Lubbe, S., P. Filzmoser, and M. Templ (2021). Comparison of zero replacement strategies for compositional data with large numbers of zeros. *Chemometrics and Intelligent Laboratory Systems 210*, 104248.

Mao, J., X. Cao, D. C. Olk, W. Chu, and K. Schmidt-Rohr (2017). Advanced solid-state nmr spectroscopy of natural organic matter. *Progress in nuclear magnetic resonance spectroscopy 100*, 17–51.

Martín-Fernández, J. and S. Thió-Henestrosa (Eds.) (2016). *Proceedings of the 6th International Workshop on Compositional Data Analysis (CoDaWork 2015)*, Springer Proceedings in Mathematics & Statistics, http://www.compositionaldata.com/codawork2015/.

Martín-Fernández, J. A. (2019). Comments on: Compositional data: the sample space and its structure, by Egozcue and Pawlowsky-Glahn. *TEST 28*(3), 653–657.

Martín-Fernández, J. A., C. Barceló-Vidal, and V. Pawlowsky-Glahn (2003). Dealing with zeros and missing values in compositional data sets using nonparametric imputation. *Mathematical Geology 35*, 253–278.

Martín-Fernández, J.-A., K. Hron, M. Templ, P. Filzmoser, and J. Palarea-Albaladejo (2015). Bayesian-multiplicative treatment of count zeros in compositional data sets. *Statistical Modelling 15*(2), 134–158.

Martín-Fernández, J. A., J. Palarea, and R. Olea (2011). Dealing with zeros. In *Compositional Data Analysis: Theory and Applications*, pp. 43–58.

Martín-Fernández, J. A., V. Pawlowsky-Glahn, J. J. Egozcue, and R. Tolosona-Delgado (2018). Advances in principal balances for compositional data. *Mathematical Geosciences 50*, 273–298.

Martino, C., J. T. Morton, C. A. Marotz, L. R. Thompson, A. Tripathi, R. Knight, and K. Zengler (2019). A novel sparse compositional technique reveals microbial perturbations. *MSystems 4*(1), 10–1128.

Mateu-Figueras, G., V. Pawlowsky-Glahn, and J. J. Egozcue (2011). The principle of working on coordinates. See Pawlowsky-Glahn and Buccianti (2011), pp. 31–42. 378 p.

Morais, J. and C. Thomas-Agnan (2021). Impact of covariates in compositional models and simplicial derivatives. *Austrian Journal of Statistics 50*, 1–15.

Muller, F. L. and M. Cuscov (2017). Alteration of the copper-binding capacity of iron-rich humic colloids during transport from peatland to marine waters. *Environmental science & technology 51*(6), 3214–3222.

Murphy, K. R., K. D. Butler, R. G. Spencer, C. A. Stedmon, J. R. Boehme, and G. R. Aiken (2010). Measurement of dissolved organic matter fluorescence in aquatic environments: an interlaboratory comparison. *Environmental science & technology 44*(24), 9405–9412.

O'Brien, J. J., J. D. O'Connell, J. A. Paulo, S. Thakurta, C. M. Rose, M. P. Weekes, E. L. Huttlin, and S. P. Gygi (2018). Compositional proteomics: Effects of spatial constraints on protein quantification utilizing isobaric tags. *Journal of Proteome Research 17*(1), 590–599. PMID: 29195270.

Oksanen, J., G. L. Simpson, F. G. Blanchet, R. Kindt, P. Legendre, P. R. Minchin, R. O'Hara, P. Solymos, M. H. H. Stevens, E. Szoecs, H. Wagner, M. Barbour, M. Bedward, B. Bolker, D. Borcard, G. Carvalho, M. Chirico, M. De Caceres, S. Durand, H. B. A. Evangelista, R. FitzJohn, M. Friendly, B. Furneaux, G. Hannigan, M. O. Hill, L. Lahti, D. McGlinn, M.-H. Ouellette, E. Ribeiro Cunha, T. Smith, A. Stier, C. J. Ter Braak, and J. Weedon (2024). *vegan: Community Ecology Package*. R package version 2.6-5.

Osterholz, H., S. Turner, L. J. Alakangas, E.-L. Tullborg, T. Dittmar, B. E. Kalinowski, and M. Dopson (2022). Terrigenous dissolved organic matter persists in the energy-limited deep groundwaters of the fennoscandian shield. *Nature Communications 13*(1), 4837.

Owen, D. D. R., V. Pawlowsky-Glahn, J. J. Egozcue, A. Buccianti, and J. M. Bradd (2016). Compositional data analysis as a robust tool to delineate hydrochemical facies within and between gas-bearing aquifers. *Water Resources Research 52*(8), 5771–5793.

Palarea-Albaladejo, J. and J. A. Martín-Fernández (2015). zcompositions – R package for multivariate imputation of left-censored data under a compositional approach. *Chemometrics and Intelligent Laboratory Systems 143*, 85–96.

Pawlowsky-Glahn, V. and A. Buccianti (Eds.) (2011). *Compositional Data Analysis: Theory and Applications*. John Wiley & Sons. 378 p.

Pawlowsky-Glahn, V. and J. J. Egozcue (2001). Geometric approach to statistical analysis on the simplex. *Stochastic Environmental Research and Risk Assessment (SERRA) 15*(5), 384–398.

Pawlowsky-Glahn, V. and J. J. Egozcue (2016). Spatial analysis of compositional data: a historical review. *Journal of Geochemical Exploration 164*, 28–32.

Pawlowsky-Glahn, V., J. J. Egozcue, and D. Lovell (2015). Tools for compositional data with a total. *Statistical Modelling 15*(2), 175–190.

Pawlowsky-Glahn, V., J. J. Egozcue, and R. Tolosana-Delgado (2007). *Lecture Notes on Compositional Data Analysis*. Girona (E): http://hdl.handle.net/10256/297.

Pawlowsky-Glahn, V., J. J. Egozcue, and R. Tolosana-Delgado (2015). *Modeling and analysis of compositional data*. Statistics in practice. John Wiley & Sons, Chichester UK. 272 pp.

Perminova, I. V., I. V. Dubinenkov, A. S. Kononikhin, A. I. Konstantinov, A. Y. Zherebker, M. A. Andzhushev, V. A. Lebedev, E. Bulygina, R. M. Holmes, Y. I. Kostyukevich, et al. (2014). Molecular mapping of sorbent selectivities with respect to isolation of arctic dissolved organic matter as measured by fourier transform mass spectrometry. *Environmental science & technology 48*(13), 7461–7468.

Qi, Y., Q. Xie, J.-J. Wang, D. He, H. Bao, Q.-L. Fu, S. Su, M. Sheng, S.-L. Li, D. A. Volmer, et al. (2022). Deciphering dissolved organic matter by fourier transform ion cyclotron resonance mass spectrometry (ft-icr ms): from bulk to fractions and individuals. *Carbon Research 1*(1), 3.

Quinn, T., I. Erb, G. Gloor, C. Notredame, M. Richardson, and T. Crowley (2019). A field guide for the compositional analysis of any-omics data. *Gigascience 8*(9), giz107.

Quinn, T. P. and I. Erb (2020, 10). Amalgams: data-driven amalgamation for the dimensionality reduction of compositional data. *NAR Genomics and Bioinformatics 2*(4), lqaa076.

Quinn, T. P., M. F. Richardson, D. Lovell, and T. M. Crowley (2017). propr: an r-package for identifying proportionally abundant features using compositional data analysis. *Scientific reports 7*(1), 1–9.

Reimann, C., P. Filzmoser, K. Fabian, K. Hron, M. Birke, A. Demetriades, E. Dinelli, A. Ladenberger, G. P. Team, et al. (2012). The concept of compositional data analysis in practice – total major element concentrations in agricultural and grazing land soils of europe. *Science of the total environment 426*, 196–210.

Riedel, T. and T. Dittmar (2014). A method detection limit for the analysis of natural organic matter via fourier transform ion cyclotron resonance mass spectrometry. *Analytical chemistry 86*(16), 8376–8382.

Rigby, R. A. and D. M. Stasinopoulos (2005). Generalized additive models for location, scale and shape. *Journal of the Royal Statistical Society Series C: Applied Statistics 54*(3), 507–554.

Rivera-Pinto, J., J. J. Egozcue, V. Pawlowsky-Glahn, R. Paredes, M. Noguera-Julian, and M. L. Calle (2018). Balances: a new perspective for microbiome analysis. *mSystems 3*(4).

Rousseeuw, P. J. (1987). Silhouettes: a graphical aid to the interpretation and validation of cluster analysis. *Journal of computational and applied mathematics 20*, 53–65.

Skinnider, M. A., J. W. Squair, and L. J. Foster (2019). Evaluating measures of association for single-cell transcriptomics. *Nature methods 16*(5), 381–386.

Stedmon, C. A., S. Markager, and R. Bro (2003). Tracing dissolved organic matter in aquatic environments using a new approach to fluorescence spectroscopy. *Marine chemistry 82*(3-4), 239–254.

Taylor, N. S., J. A. Kirwan, N. D. Yan, M. R. Viant, J. M. Gunn, and J. C. McGeer (2016). Metabolomics confirms that dissolved organic carbon mitigates copper toxicity. *Environmental toxicology and chemistry 35*(3), 635–644.

Templ, M. and B. Templ (2020). Analysis of chemical compounds in beverages–guidance for establishing a compositional analysis. *Food chemistry 325*, 126755.

Thompson, A. M., K. G. Stratton, L. M. Bramer, N. S. Zavoshy, and L. A. McCue (2021). Fourier transform ion cyclotron resonance mass spectrometry (ft-icr-ms) peak intensity normalization for complex mixture analyses. *Rapid Communications in Mass Spectrometry 35*(9), e9068.

Tolosana-Delgado, R. (2012). Uses and misuses of compositional data in sedimentology. *Sedimentary Geology 280*, 60–79.

Tranvik, L. J. (1992). Allochthonous dissolved organic matter as an energy source for pelagic bacteria and the concept of the microbial loop. *Hydrobiologia 229*, 107–114.

Wong, R. G., J. R. Wu, and G. B. Gloor (2016). Expanding the unifrac toolbox. *PloS one 11*(9), e0161196.

Zuur, A. F., E. N. Ieno, and C. S. Elphick (2010). A protocol for data exploration to avoid common statistical problems. *Methods in ecology and evolution 1*(1), 3–14.

5 Appendix

Useful books and papers for interested readers.

1. Books

    - The Statistical Analysis of Compositional Data (Aitchison, 1986)
    - Lecture Notes on Compositional Data Analysis (Pawlowsky-Glahn et al., 2007)
    - Compositional Data Analysis (Pawlowsky-Glahn and Buccianti, 2011)
    - Analyzing Compositional Data with R (Boogaart and Tolosana-Delgado, 2013)
    - A Concise Guide to Compositional Data Analysis (Aitchison, 2005)
    - Modeling and Analysis of Compositional Data (Pawlowsky-Glahn et al., 2015)
    - Compositional Data Analysis (CoDaWork 2015) (Martín-Fernández and Thió-Henestrosa, 2016)
    - Applied Compositional Data Analysis With Worked Examples in R (Filzmoser et al., 2018)
    - Compositional Data Analysis (Greenacre, 2021)

2. Reviews/Perspectives

    - Compositional Data Analysis: Where Are We and Where Should We Be Heading? (Aitchison and Egozcue, 2005)
    - The single principle of compositional data analysis, continuing fallacies, confusions and misunderstandings and some suggested remedies (Aitchison, 2008)
    - Tools for compositional data with a total (Pawlowsky-Glahn et al., 2015)
    - Spatial analysis of compositional data: A historical review (Pawlowsky-Glahn and Egozcue, 2016)
    - The Mathematics of Compositional Analysis (Barceló-Vidal and Martín-Fernández, 2016)
    - Compositional data: the sample space and its structure (Egozcue and Pawlowsky-Glahn, 2019)

- 40 years after Aitchison's article "The statistical analysis of compositional data". Where we are and where we are heading (Coenders et al., 2023)

3. Tutorials

- Univariate statistical analysis of environmental (compositional) data: Problems and possibilities (Filzmoser et al., 2009)
- The bivariate statistical analysis of environmental (compositional) data (Filzmoser et al., 2010)
- The concept of compositional data analysis in practice - Total major element concentrations in agricultural and grazing land soils of Europe (Reimann et al., 2012)
- Compositional data analysis as a robust tool to delineate hydrochemical facies within and between gas-bearing aquifers (Owen et al., 2016)
- Microbiome Datasets Are Compositional: And This Is Not Optional (Gloor et al., 2017)
- Compositional Proteomics: Effects of Spatial Constraints on Protein Quantification Utilizing Isobaric Tags (O'Brien et al., 2018)
- A field guide for the compositional analysis of any-omics data, Thomas P Quinn, Ionas Erb, Greg Gloor, Cedric Notredame, Mark F Richardson, Tamsyn M Crowley, GigaScience, 2019 (Quinn et al., 2019)
- Analysis of Chemical Compounds in Beverages- Guidance for Establishing a Compositional Analysis (Templ and Templ, 2020)
- The selection and analysis of fatty acid ratios: A new approach for the univariate and multivariate analysis of fatty acid trophic markers in marine pelagic organisms (Graeve and Greenacre, 2020)
- Exploring geochemical data using compositional techniques: A practical guide (Egozcue et al., 2024)

Supporting Information for: Reframing natural organic matter research through compositional data analysis

Morimaru Kida[1,*], Julian Merder[2,a], Thorsten Dittmar[3,4], Vera Pawlowsky-Glahn[5], and Juan José Egozcue[6]

[1]Soil Science Laboratory, Graduate School of Agricultural Science, Kobe University, 1-1 Rokkodai, Nada, Kobe, Hyogo 657-8501, Japan,
[2]Department of Global Ecology, Carnegie Institution for Science, 260 Panama Street, Stanford, CA 94305, USA
[3]Institute for Chemistry and Biology of the Marine Environment (ICBM), School of Mathematics and Science, University of Oldenburg, Oldenburg, Germany
[4]Helmholtz Institute for Functional Marine Biodiversity at the University of Oldenburg (HIFMB), Oldenburg, Germany
[5]Department of Computer Sciences, Applied Mathematics, and Statistics, Universitat de Girona, Campus Montilivi, P4, 17003 Girona, Spain
[6]Department of Civil and Environmental Engineering, Universitat Politécnica de Catalunya, Jordi Girona 1-3, Mod. C2, 08034 Barcelona, Spain
[a]Present address: School of Biological Sciences, University of Canterbury, Private Bag 4800, Christchurch 8140, New Zealand

October 13, 2025

*__Corresponding Author:__ **Morimaru Kida**, Soil Science Laboratory, Graduate School of Agricultural Science, Kobe University, 1-1 Rokkodai, Nada, Kobe, Hyogo 657-8501, Japan. morimaru.kida@people.kobe-u.ac.jp

Table of contents:

1 Supplementary Introduction

1.1 From proportionality of, to distances between, compositions

CoDa can be multiplied by a positive constant without changing its meaning and conveyed information. For instance, proportions between peaks as $(0.1, 0.7, 0.2)$ can be expressed in percentages as $(10, 70, 20)\%$. This corresponds to Aitchison's *principle of scale invariance* (Aitchison, 1986) and to the idea that these two compositions, being proportional, are equivalent. This idea of equivalence collides with the possibility of using the Euclidean distance between compositions since it changes by a factor of 100 from proportions to percentages. This inconvenience can be circumvented by forcing the closure of compositions so that their components add to a fixed arbitrary positive constant (e.g. 1, 100, 10^6). However, this possibility is still unsatisfactory since one expects that considering a smaller number of peaks, a subcomposition, the distance between two compositions is less than or equal to, that of the original compositions with a larger number of peaks. For instance, compare $(0.1, 0.7, 0.2)$ to $(0.5, 0.4, 0.1)$; their Euclidean distance is 0.51. Suppressing the last part and closing it to 1, results in two 2-part compositions $(0.125, 0.875)$, $(0.556, 0.444)$ whose Euclidean distance is 0.61, thus an increasing distance for a smaller number of parts against the initial assumption (against the principle of *subcompositional dominance*). Then, a distance between compositions should be invariant under change of scale (Aitchison et al., 2000). Furthermore, a distance for CoDa should be invariant when a shift is applied. This requires the identification of a shift for compositions. This shift was introduced in Aitchison (1982) and named *perturbation*. It consists of a multiplicative change of each part in the composition. For instance, the composition $(0.1, 0.7, 0.2)$ could change to $(0.1 \times 0.95, 0.7 \times 1.03, 0.2 \times 1)$ by a perturbation $(0.95, 1.03, 1)$ which is again a composition. In many scenarios, this perturbation is described as changes of -5%, 3% for the first two parts respectively and no change for the third one. These requirements on the distances applicable to CoDa were discussed in Aitchison et al. (2000).

Another important point in the analysis of CoDa is that any composition can be represented in the simplex by taking closure (constant sum of parts). In the simplex, perturbation and *powering* are defined as follows. For $\mathbf{x} = (x_1, x_2, \ldots, x_D)$, $\mathbf{y} = (y_1, y_2, \ldots, y_D)$ compositions with D-parts, and α a real constant, perturbation and powering are

$$\mathbf{x} \oplus \mathbf{y} = \mathcal{C}(x_1 y_1, x_2 y_2, \ldots, x_D y_D) \quad , \quad \alpha \odot \mathbf{x} = \mathcal{C}(x_1^\alpha, x_2^\alpha, \ldots, x_D^\alpha) \, ,$$

where $\mathcal{C}$ denotes closure, $\oplus$ and $\odot$ are the operations between compositions. Note that the use of closure is optional, as it is only a selection of the representative of

the equivalence class of compositions. Perturbation plays the role of addition of compositions and a difference perturbation allows computation of deviations between compositions $\mathbf{x} \ominus \mathbf{y} = \mathbf{x} \oplus ((-1) \odot \mathbf{y})$ what is just a rationing of the parts in $\mathbf{x}$ and $\mathbf{y}$. The set of all D-part compositions with perturbation and powering is a $(D-1)$-dimensional linear vector space. This theoretical result has consequences in practice. For instance, the compositional average (avec) of n compositions is written as

$$\text{avec}(\mathbf{x}_i, i = 1,2,\ldots,n) = \frac{1}{n} \odot \bigoplus_{i=1}^{n} \mathbf{x}_i \ ,$$

which can be computed as the geometric mean of each part across the compositional sample.

A proper distance for CoDa was proposed in Aitchison (1983) and confirmed e.g. in Aitchison et al. (2000) and Gloor et al. (2017). This distance, now named *Aitchison distance*, is computed as follows:

$$\mathrm{d}_A(\mathbf{x},\mathbf{y}) = \left(\sum_{i=1}^{D} (\mathrm{clr}_i(\mathbf{x}) - \mathrm{clr}_i(\mathbf{y}))^2 \right)^{1/2} , \tag{1}$$

where the centered log-ratio (clr) of a composition is used:

$$\mathrm{clr}(\mathbf{x}) = \left(\ln \frac{x_1}{\mathrm{g_m}(\mathbf{x})}, \ln \frac{x_2}{\mathrm{g_m}(\mathbf{x})}, \ldots, \ln \frac{x_D}{\mathrm{g_m}(\mathbf{x})} \right) , \tag{2}$$

where $\mathrm{g_m}$ denotes the geometric mean of terms in the argument. Note that $\mathrm{d}_A(\mathbf{x},\mathbf{y})$ in Equation (1) is the Euclidean distance of the corresponding clr vectors. It can be proven that the Aitchison distance comes from an inner product in the set of compositions. Consequently, the D-part simplex is a $(D-1)$-dimensional Euclidean space (Pawlowsky-Glahn and Egozcue, 2001; Billheimer et al., 2001). This result has important consequences. The well-known properties of Euclidean spaces like parallel and orthogonal straight lines, orthogonal projections, norm and distance of compositions, orthogonal bases, and coordinates are available. Once some orthogonal basis is chosen, and the compositions are represented using the respective orthogonal coordinates, all statistical and geometric procedures and methods designed for real random variables can be applied to the orthogonal coordinates. This is termed the *Principle of Working in Coordinates* (Mateu-Figueras et al., 2011). The design of orthogonal basis for compositions can be based on the researcher's preferences (Egozcue et al., 2003; Egozcue and Pawlowsky-Glahn, 2005) or driven by the compositional data at hand using the CoDa-principal component analysis (Aitchison, 1983; Aitchison and Greenacre, 2002). Any assignation of orthogonal coordinates to CoDa is named isometric log-ratio (ilr) or orthonormal log-ratio (olr) (Egozcue and Pawlowsky-Glahn, 2019; Martín-Fernández, 2019).

1.2 Equations mentioned in the main manuscript

Balance: The balance between two groups of parts in a composition, $(x_1,\ldots,x_r)$ and $(z_1,\ldots,z_s)$, is defined as (Egozcue and Pawlowsky-Glahn, 2005):

$$B(x_1,\ldots,x_r/y_1,\ldots,y_s) = \sqrt{\frac{rs}{r+s}} \log \frac{\mathrm{g_m}(x_1,\ldots,x_r)}{\mathrm{g_m}(y_1,\ldots,y_s)}\,, \tag{3}$$

where $\mathrm{g_m}$ is the geometric mean of its arguments, $\mathrm{g_m}(x_1,\ldots,x_r) = (x_1 \cdot \ldots \cdot x_r)^{1/r}$. The square root term is a normalizing constant to make comparable balances whose groups of parts have different number of elements.

Robust centered log-ratio (rclr)**:** Robust clr is defined as (Martino et al., 2019):

$$\mathrm{rclr}(\mathbf{x}) = \left(\ln \frac{x_i}{\mathrm{g_m}(\mathbf{x}>0)}\right)_{i=1,\ldots,D} \text{ with } \mathrm{g_m}(\mathbf{x}>0) = \prod_{x_i>0} x_i^{1/D}. \tag{4}$$

2 Supplementary Discussion

2.1 Correlation by groups

When the number of variables is small, the negative correlation bias tends to increase as the number of variables decreases. An empirical example comes from the analysis of 16S rRNA gene sequence data from the Human Microbiome Project, where sample diversity (i.e., alpha diversity) strongly predicted the negative correlation bias, which diminished with increasing diversity (Friedman and Alm, 2012). In the most extreme case, when a composition consists of only two parts summing up to unity, they exhibit a perfect negative correlation with a correlation coefficient of -1.0. With three parts, it remains highly unlikely for any pair to show a positive correlation. However, there is currently no consensus on when this bias behaves unpredictably. For compound classes with seven parts (Fig. 2), should the sum constraint be particularly evident in correlation analysis? A simple way to check this is by subsetting the data (i.e., removing one or more parts), followed by re-normalisation (*closing*) of the remaining data (*subcomposition*) and comparing correlations before and after subsetting. Table S1 shows the effects of removing the CHO class, where the correlations between the compound classes changed most substantially. The largest difference in correlation coefficients before and after subsetting occurred between CHON and CHOS (Table S1). The near-absence of correlation between these parts in the full composition became a strong negative correlation in the subcomposition. This indicates that closing the data to 1 (i.e., representation by relative abundance) introduces an artefact in component associations. Consequently, associations between components can vary depending on the number of components considered (i.e., *subcompositionally not coherent*). The problem is that in practice, you always measure relative abundances, as the whole object to be measured is not attainable, and if it were, it would still be relative to the total amount.

Table S1: **The difference in the Pearson correlation coefficients before and after subsetting (removing CHO) of the data.** The lower triangle shows the difference in the correlation coefficients after subsetting minus those before subsetting, while the upper triangle shows the correlation coefficients before and after subsetting, respectively.

	CHON	CHOS	CHOP	CHONS	CHONP	CHOSP
CHON	1	$0.05 \rightarrow -0.98$	$0.36 \rightarrow 0.36$	$0.26 \rightarrow -0.76$	$0.24 \rightarrow -0.23$	$-0.02 \rightarrow 0.16$
CHOS	-1.03	1	$-0.31 \rightarrow -0.53$	$0.9 \rightarrow 0.7$	$0.21 \rightarrow 0.19$	$-0.24 \rightarrow -0.29$
CHOP	0	-0.22	1	$-0.16 \rightarrow -0.37$	$0.28 \rightarrow 0.14$	$0.69 \rightarrow 0.7$
CHONS	-1.02	-0.2	-0.21	1	$0.17 \rightarrow 0.02$	$-0.13 \rightarrow -0.23$
CHONP	-0.47	-0.02	-0.14	-0.15	1	$0.24 \rightarrow 0.25$
CHOSP	0.18	-0.05	0.01	-0.1	0.01	1

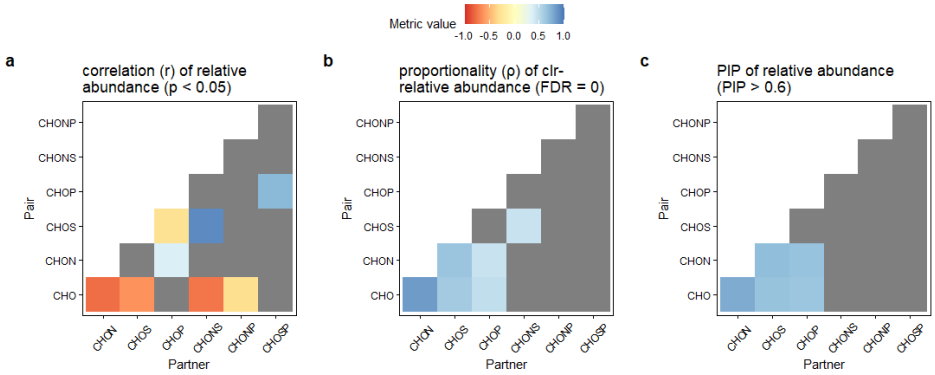

Figure S1: **Comparisons of association of compound classes using non-compositional and compositional methods.** (a) Pearson correlation coefficients (r) of the relative abundance, (b) symmetric proportionality coefficients (ρ) of the clr-transformed relative abundance, and (c) proportionality index of parts (PIP) of the relative abundance. The grey colour indicates the pairs with no associations; (a) p-value ≥ 0.05, (b) $\rho < 0.35$, a threshold chosen to keep the false discovery rate as 0% (Quinn et al., 2017), and (c) PIP < 0.60, tentatively assigned as not proportional. Note that a clr component is not the variable *per se* but a logratio of the variable and the geometric mean of all variables. Thus, it should be interpreted with respect to all the other variables connected through the geometric mean.

Figure S1 compares the association of compound classes using non-compositional and compositional methods. For a non-compositional method, Pearson correlations were computed for the relative abundance among compound classes. For compositional methods, symmetric proportionality coefficients (ρ) (Erb and Notredame, 2016) and proportionality index of parts (PIP) (Egozcue and Pawlowsky-Glahn, 2023) were calculated for the relative abundance among compound classes (see Table 1 in the main manuscript for the interpretation of these measures). The clr transformation was applied before ρ was calculated, while PIP produces the identical results with or without the ρ transformation. Notably, the most proportional pair (CHO vs CHON; $\rho = 0.82$, PIP $= 0.75$) (Fig. S1b, c) exhibited the strongest negative correlation on a relative scale ($r = -0.79$)(Fig. S1a), illustrating a clear example of negative bias. These two molecular classes were highly dominant, collectively accounting for $71 - 96\%$ of the relative abundance (Fig. 2). Therefore, a change in one class would tend to force the other in the opposite direction. CHO had predominantly negative correlations with the other classes (Fig. S1a) because of its dominance in the composition. Importantly, negative correlations on a relative scale do not necessarily imply negative correlations in absolute abundances within the lakes studied. The problem is that there is no theoretical method to distinguish these negative correlations that arise structurally from those that are true negative

correlations driven by the underlying processes, and ”true” correlations can not be derived from subcompositionally incoherent coefficients such as Pearson's r.

2.2 PCA by groups

Figure S2 compares PCAs of the original relative abundance and clr-transformed abundance of compound classes. The ordinary PCA was conducted (assuming an absolute scale) after normalisation and centring of variables (i.e., based on correlation matrix), while normalisation was not necessary for compositional PCA (CoDa-PCA) due to the scale-invariant nature of the clr-transformation. A few zeros were imputed accounting for the relative covariance structure by a robust Expectation-Maximisation algorithm before clr computation, using a *lrEM()* function in the *zCompositions* package (Palarea-Albaladejo and Martín-Fernández, 2015). As a reference, samples were colour-coded based on predetermined clusters derived from the frequency distributions of double-bond equivalent of molecular formulae between samples (Kida et al., 2023), which did not use peak intensity information to avoid compositional problems. In the standard PCA based on original relative abundance (Fig. S2a), a typical phenomenon when there is a dominant variable(s) in the dataset was observed – most variables showed negative correlations with the most dominant CHO class. This is a clear example of the sum constraint (Otero et al., 2005), already observed in correlation analysis (Fig. S1a). In the worst case, differences between less abundant variables can be masked and mistakenly treated as similar despite their potential differences. In contrast, CoDa-PCA shows that variables were more evenly distributed and variation in the dataset was most strongly driven by the most varying classes such as CHONS, CHONP, and CHOSP (Fig. S2b). In terms of sample distribution, one notable difference was that the two samples of cluster 3, collected at different depths in a hypersaline lake (Kida et al., 2023), were plotted in the middle of the ordinary PCA but at the cloud edge of the sample characterised by the CHONP class in CoDa-PCA. Because these hypersaline samples had distinct molecular characteristics from other freshwater lakes (Kida et al., 2023), CoDa-PCA better summarised the sample differences than ordinary PCA.

The interpretation of CoDa-PCA differs from the ordinary one. First, the lengths of the arrows in the covariance biplot are approximations of the standard deviation of the corresponding clr-transformed variable, $\mathrm{clr}_i(\mathbf{x})$ (Aitchison and Greenacre, 2002). The standard deviation of clr-transformed variables tends to be larger for variables with a high relative variation (coefficient of variation). Therefore, assessing whether contributions from less abundant variables are not overemphasised due to low analytical precision is important. In our current example, we previously confirmed that the precision of duplicate measurements for compound classes, defined

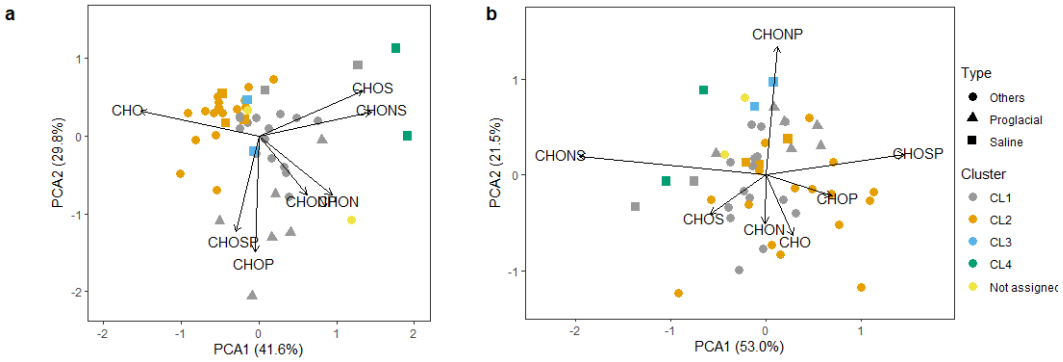

Figure S2: **Comparison of principal component analysis (PCA) of the original relative abundance (a) and** clr**-transformed abundance of compound classes.** Both biplots are correlation (scaling 2) (Legendre and Legendre, 2012) or covariance (Aitchison and Greenacre, 2002) biplots, where relationships between variables are preserved. Predetermined clustering is based on the frequency distributions of the double bond equivalent of molecular formulae between samples (Kida et al., 2023) and shown for reference.

as the scaled relative difference, was generally better than 5% and never exceeded 10% (Kida et al., 021a). Furthermore, CHONS made the largest contribution to CoDa-PCA than one-order less CHONP and CHOSP classes (Figs. 1 and S2), assuring that this concern does not apply. Second, the distances (links) between the vertices of the i-th and the k-th clr-variable are approximations of the standard deviation of the corresponding logratio, $\ln(x_i/x_k)$ (Aitchison and Greenacre, 2002). For example, the largest link between CHONS and CHOSP indicates that there is the largest relative variation in these two compound classes across the dataset. The second point highlights the fundamental elements of a CoDa-biplot, where the links between arrows are relevant. If the vertices of the two arrows nearly coincide, it indicates that the variance $\ln(x_i/x_k)$ is nearly zero and the ratio x_i/x_k is nearly constant, indicating proportionality between these variables. Aitchison and Greenacre (2002) gives thorough interpretations and theories of CoDa-PCA biplots. The relatively high proportionality between CHO and CHON (Fig. S1b, c) can be seen here as the shortest distance between the vertices of their arrows (Fig. S2b).

2.3 additive logratio

We present an approach that can simplify CoDa analysis for practitioners working with high-dimensional datasets (say, $D > 10^2$, where D is the number of parts), such as FT-ICR MS data. This approach employs the simplest logratio transformation, alr, while minimising its limitation on non-isometry (Table 1 in the main manuscript) (details in Greenacre et al. (2021)). Non-isometry can be minimised by

selecting a reference that maximises the Procrustes correlation between the alr geometry and the exact logratio (Aitchison) geometry. For high-dimensional datasets, numerous potential references are available (Greenacre et al., 2021). Another criterion for selecting the reference is that its relative abundance should remain as constant as possible across samples. Because dividing each component by an almost constant reference value shifts all logratios by nearly the same amount, the resulting logratio can be practically interpreted as the numerator on a logarithmic scale (Greenacre et al., 2021), a property not permitted in other logratio transformations. Figure S3 illustrates the distances between samples computed from alrs

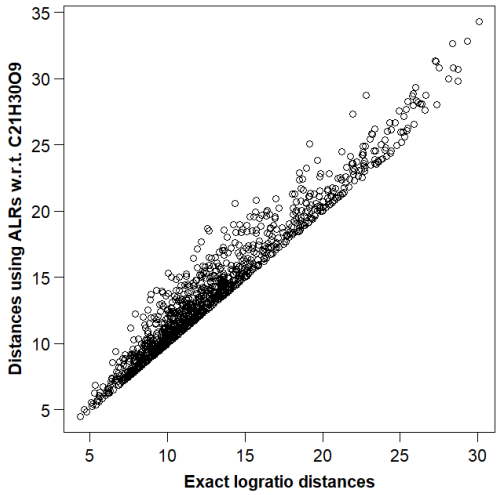

Figure S3: **Between-sample distances for the Antarctic lake dataset** (Kida et al., 2023) **based on the** alr**'s with reference molecular formula C21H30O9 versus the exact logratio distances, corresponding to the Procrustes correlation of 0.9832.** This reference molecular formula has the 103rd highest relative abundance among the 1,214 common molecular formulae.

plotted against the corresponding exact logratio distances based on all pairwise logratios, or equivalently, on all clr's, showing the near-isometric nature of the selected alr variables. The chosen reference was the molecular formula C21H30O9, which had the second-highest Procrustes correlation (0.9832) and the third-lowest variance of log-transformed relative abundance (0.00956, range between -6.611 and -6.051). Consequently, PCA results derived from the selected set of alrs resembled those obtained from exact logratio distances based on all pairwise logratios (note that logratio analysis is the PCA of all pairwise logratios, which is equivalent to the PCA of all clrs), with only minor differences in certain lakes (e.g., L42, the hypersaline Lake Suribachi) (Fig. S4). These findings demonstrate that the alr transfor-

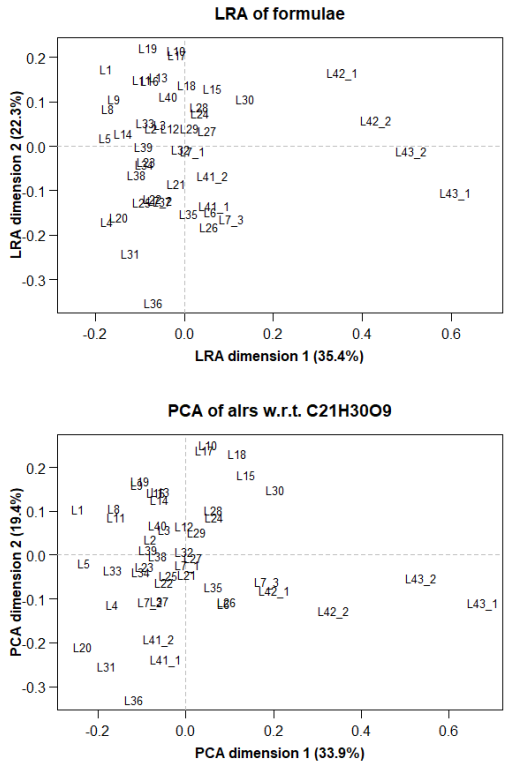

Figure S4: **Logratio analysis of the Antarctic lake dataset** (Kida et al., 2023)**, aiming to explain the total logratio variance based on all pairwise logratios of molecular formulae (top), and principal component analysis of** alr**'s with the reference molecular formula C21H30O9 (down), showing a geometry similar to the exact logratio geometry (Procrustes correlation = 0.9832).** The different numbers after L indicate different lakes, while the numbers after underscore indicate different sampling depths within the same lake.

mation can, in some cases, provide a valid solution for analysing high-dimensional compositional datasets, thereby greatly simplifying CoDa analysis for practitioners. However, we note that it needs to be investigated for each new application, and if a suitable reference that satisfies the first criterion (geometry matching) cannot be found, other logratio transformations (such as clr and ilr) must be used for analysis of CoDa. We also note that the alr distances were, although highly similar (by Procrustes correlation of 0.9832), systematically larger than the exact distances (Fig. S3), potentially leading to spurious results regarding relationships between samples (like the case in Lake Suribachi).

At this point, a word of caution is needed. The use of the alr approach has mul-

tiple pitfalls and only one apparent advantage: the interpretation of the coordinates, which are logratios of single parts over the reference. But in this approach, a contradiction is implicit: assuming subcompositional coherence, we can add a constant part without altering inferences. Now take this constant part as reference in the alr. Then the alr analysis is reduced to the analysis of the log of parts in $\mathcal{R}_+$, which is known to be scale dependent (Pawlowsky-Glahn et al., 2015). Moreover, this approach tries to hide the fact that any pairwise logratio can be statistically analysed, independently of the fact that this logratio appears or not as a coordinate in the selected transformation.

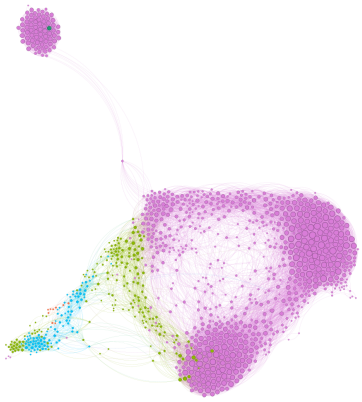

Figure S5: **Network analysis of the common peaks of the exemplary Antarctic lake dataset** (Kida et al., 2023) **based on the symmetric proportionality coefficient** ρ. To control for the false-discovery rate (FDR), a cutoff of $\rho > 0.75$ (FDR$= 0\%$) was selected based on permutation of FDR for ρ values ranging between $0-1$ (Quinn et al., 2019), resulting in the retention of 1168 molecular formulae and 22173 pairs. Peaks are represented by points (nodes) and highly proportional pairs are linked by non-directional lines (edges). Nodes are colour-coded based on the nitrogen content: pink $= 0$, light green $= 1$, light blue $= 2$, orange $= 3$. The node size is proportional to the number of edges it has. A small "island" located at the top-left corner consists of S-containing peaks that were completely absent in other nodes. The network layout algorithm was by ForceAtlas2 (Jacomy et al., 2014). Nodes with a single edge (leaves) were removed for parsimony.

References

Aitchison, J. (1982). The statistical analysis of compositional data (with discussion). *Journal of the Royal Statistical Society, Series B (Statistical Methodology) 44*(2), 139–177.

Aitchison, J. (1983). Principal component analysis of compositional data. *Biometrika 70*(1), 57–65.

Aitchison, J. (1986). *The Statistical Analysis of Compositional Data*. Monographs on Statistics and Applied Probability. London (UK): Chapman & Hall Ltd., London (UK). (Reprinted in 2003 with additional material by The Blackburn Press). 416 p.

Aitchison, J., C. Barceló-Vidal, J. A. Martín-Fernández, and V. Pawlowsky-Glahn (2000). Logratio analysis and compositional distance. *Mathematical Geology 32*(3), 271–275.

Aitchison, J. and M. Greenacre (2002). Biplots for compositional data. *Journal of the Royal Statistical Society, Series C (Applied Statistics) 51*(4), 375–392.

Billheimer, D., P. Guttorp, and W. Fagan (2001). Statistical interpretation of species composition. *Journal of the American Statistical Association 96*(456), 1205–1214.

Egozcue, J. J. and V. Pawlowsky-Glahn (2005). Groups of parts and their balances in compositional data analysis. *Mathematical Geology 37*(7), 795–828.

Egozcue, J. J. and V. Pawlowsky-Glahn (2019). Compositional data: the sample space and its structure. *TEST 28*(3), 599–638.

Egozcue, J. J. and V. Pawlowsky-Glahn (2023). Subcompositional coherence and a novel proportionality index of parts. *SORT 47*(2), 229–244.

Egozcue, J. J., V. Pawlowsky-Glahn, G. Mateu-Figueras, and C. Barcelo-Vidal (2003). Isometric logratio transformations for compositional data analysis. *Math. Geol. 35*, 279–300.

Erb, I. and C. Notredame (2016). How should we measure proportionality on relative gene expression data? *Theory in Biosciences 135*(1-2), 21–36.

Friedman, J. and E. J. Alm (2012). Inferring correlation networks from genomic survey data. *PLoS Computational Biology 8*(9), e1002687.

Gloor, G. B., J. M. Macklaim, V. Pawlowsky-Glahn, and J. J. Egozcue (2017). Microbiome datasets are compositional: and this is not optional. *Frontiers Microbiology 8*, 2224.

Greenacre, M., M. Martínez-Álvaro, and A. Blasco (2021). Compositional data analysis of microbiome and any-omics datasets: a validation of the additive logratio transformation. *Frontiers in microbiology 12*, 727398.

Jacomy, M., T. Venturini, S. Heymann, and M. Bastian (2014). Forceatlas2, a continuous graph layout algorithm for handy network visualization designed for the gephi software. *PloS one 9*(6), e98679.

Kida, M., N. Fujitake, T. Kojima, Y. Tanabe, K. Hayashi, S. Kudoh, and T. Dittmar (2021a). Dissolved organic matter processing in pristine antarctic streams. *Environmental Science & Technology 55*(14), 10175–10185.

Kida, M., J. Merder, N. Fujitake, Y. Tanabe, K. Hayashi, S. Kudoh, and T. Dittmar (2023). Determinants of microbial-derived dissolved organic matter diversity in antarctic lakes. *Environmental Science & Technology 57*(13), 5464–5473.

Legendre, P. and L. Legendre (2012). Chapter 9 - ordination in reduced space. In P. Legendre and L. Legendre (Eds.), *Numerical Ecology*, Volume 24 of *Developments in Environmental Modelling*, pp. 425–520. Elsevier.

Martín-Fernández, J. A. (2019). Comments on: Compositional data: the sample space and its structure, by Egozcue and Pawlowsky-Glahn. *TEST 28*(3), 653–657.

Martino, C., J. T. Morton, C. A. Marotz, L. R. Thompson, A. Tripathi, R. Knight, and K. Zengler (2019). A novel sparse compositional technique reveals microbial perturbations. *MSystems 4*(1), 10–1128.

Mateu-Figueras, G., V. Pawlowsky-Glahn, and J. J. Egozcue (2011). The principle of working on coordinates. In V. Pawlowsky-Glahn and A. Buccianti (Eds.), *Compositional Data Analysis: Theory and Applications*, pp. 31–42. John Wiley & Sons. 378 p.

Otero, N., R. Tolosana-Delgado, A. Soler, V. Pawlowsky-Glahn, and A. Canals (2005). Relative vs. absolute statistical analysis of compositions: a comparative study of surface waters of a mediterranean river. *Water research 39*(7), 1404–1414.

Palarea-Albaladejo, J. and J. A. Martín-Fernández (2015). zcompositions – R package for multivariate imputation of left-censored data under a compositional approach. *Chemometrics and Intelligent Laboratory Systems 143*, 85–96.

Pawlowsky-Glahn, V. and J. J. Egozcue (2001). Geometric approach to statistical analysis on the simplex. *Stochastic Environmental Research and Risk Assessment (SERRA) 15*(5), 384–398.

Pawlowsky-Glahn, V., J. J. Egozcue, and D. Lovell (2015). Tools for compositional data with a total. *Statistical Modelling 15*(2), 175–190.

Quinn, T. P., I. Erb, G. Gloor, C. Notredame, M. F. Richardson, and T. M. Crowley (2019). A field guide for the compositional analysis of any-omics data. *GigaScience 8*(9), giz107.

Quinn, T. P., M. F. Richardson, D. Lovell, and T. M. Crowley (2017). propr: an r-package for identifying proportionally abundant features using compositional data analysis. *Scientific reports 7*(1), 1–9.